6. Drug Transport through the Chimeric *m*-Hepatocyte Membrane

Drug transport in the liver is largely performed by two systems: extrahepatic-to-hepatic transport using transporters such as organic cation transporter 1 (OCT1), organic anion transporting polypeptide (OATP) 1B1, and OATP1B3; and hepatic-to-bile duct transport using adenosine 5′-triphosphate-binding cassette (ABC) proteins, including P-glycoprotein, bile salt export pump (BSEP/ABCB11), breast cancer resistance protein (BCRP/ABCG2), and multidrug resistance-associated protein 2 (MRP2) [36]. The former transporters are located on the sinusoidal membrane and are responsible for the uptake of drugs into hepatocytes; the latter are on the canalicular membrane and are responsible for biliary excretion of the metabolites. The *h*-genes of these transporting systems were preferentially expressed compared with the *m*-counterpart genes in chimeric mice with RIs >60% [36]. Cefmetazole (CMZ), a cephalosporin antibiotic, is excreted without any chemical modification, through urinary and biliary pathways. The urinary pathway is dominant in humans [37], whereas rats [38] and mice [36] use the biliary pathway. Before receiving *h*-hepatocytes, the host mice excreted CMZ primarily through the biliary pathway, but the urinary pathway was dominant in chimeric mice with RIs >60% [36].

The *h*-ABCB4 transporters have been characterized in relation to fibrate-metabolism [39]. In addition, we examined the expression levels of 21 *h*-transporter genes, including members of the ABC, solute carrier (SLC), and OATP families, in the livers of chimeric mice with RIs ranging from 71 to 89%, with respect to the levels in donor livers [16]. For 62% of the tested genes, the expression ratios in the chimeric livers were 0.35 to 0.75. From these limited data, it appears that most of the *h*-type transporter genes were expressed in the chimeric *m*-liver.

7. Infectivity of Chimeric Mice with *h*-Hepatitis Viruses

h-Liver diseases caused by HBV and HCV, especially HCV, are targets for the discovery of efficient antivirus drugs, worldwide [40]. However, the development of effective therapeutics has been hampered by the lack of useful in vitro and in vivo models of viral replication. For example, cultured *h*-hepatocytes are not appropriate as recipient cells for viral propagation, and rodents are not useful animal models because of the strict species specificity of viral infection [41]. Viral infectivity and propagative potential in the *h*/*m*-chimeric mouse would be persuasive evidence for concluding that it was actually "humanized." A research group led by Kneteman first challenged chimeric mice with an inoculation of HCV-infected *h*-serum, which produced a virus-infected model mouse [7]. Owing to their substantial advantage in both magnitude and duration of *h*-hepatocyte engraftment, homozygous animals were superior to their hemizygous counterparts in this regard. Initial increases in total viral load were up to 1950-fold, with replication confirmed by the detection of negative-strand viral RNA in transplanted livers. HCV viral proteins were localized to *h*-hepatocyte nodules, and infection was serially passed through three generations of mice, confirming both synthesis and release of infectious viral particles. Using *h*-hepatocyte-chimeric Rug-2-knockout mice as test animals, Dandri et al. was the first to succeed in producing in vivo HBV infection [6].

We studied HBV infectivity in the chimeric mice [42]. After mice were inoculated with *h*-serum containing HBV, a high level of viremia occurred in mice for up to 22 weeks. Passage experiments showed that the serum of these mice contained infectious HBV. As shown previously for HCV, the level of HBV viremia tended to be high in mice with a continuously high RI. Furthermore, lamivudine, an anti-HBV drug, effectively reduced the level of viremia in the infected mice. Thus, the chimeric mouse may be an ideal model in which we can develop and evaluate anti-*h*-hepatitis virus drugs.

8. The *h*/*m*-Chimeric Mouse as an Animal Model for the Study of *h*-Type Peroxisome Proliferator-Activated Receptors

8.1. Drug Metabolism under The Control of Ligand-Activated Receptors. Biochemical systems in the liver manage not only endogenous (homobiotic), but also xenobiotic molecules. These molecules are first recognized by specific protein receptors on the hepatocyte surface. In general, the binding of a ligand to its receptor generates a signal that ultimately changes gene expression, producing a cellular response. Hepatocytes possess four types of receptors [16], all of which are ligand-activated transcriptional regulators: CAR; PXR [also called steroid X receptor (SXR)]; peroxisome proliferator-activated receptor (PPAR); and aryl hydrocarbon receptor (AHR). The first three belong to the nuclear receptor (NR) superfamily, which consists of seven subfamilies, 1 to 6 and 0 [43]. AHR is a member of the Per-AhR/Arnt-Sim homology sequence (PAS)/basic helix-loop-helix (HLH) superfamily, which also represents the period regulator of circadian rhythm (PER), Ah receptor nuclear translocator (ARNT), and single-minded regulator of midline cell differentiation.

Historically, the roles of PPARs have been studied using liver. They belong to NR subfamily 1, along with thyroid hormone receptor, retinoic acid receptor (RAR), and vitamin D receptor (VDR). As transcription factors, these receptors share a similar process. They are activated by ligand binding; form heterodimers, usually with the retinoid X receptor (RXR); translocate to the nucleus; bind to a *cis*-acting XRE consisting of a direct repeat of two hexanucleotides, separated by one or two nucleotides, in the promoter region of the target gene; and enhance target gene expression [17]. Generally, in the absence of ligand, subfamily 1 NR heterodimers are bound to co-repressor proteins and repress transcription when bound to the *cis*-acting element [44]. Upon ligand binding, the receptor dissociates from the co-repressors and associates with coactivator proteins, which enables the NRs to promote gene expression.

Three PPAR subtypes are currently known [45]: PPARα (or NR1C1), PPARβ/δ (NR1C2), and PPARγ (NR1C3). When continuously exposed to certain xenobiotics such as hypolipidemic drugs, plasticizers, and herbicides, which have little apparent structural relationship, rats and mice may show hepatic peroxisome proliferation (increase in volume and number) leading to hepatic tumors; this suggests a correlation between the stimulation of genes for fatty acid β- and ω-oxidation enzymes and the hepatic neoplastic process [46, 47]. Reddy and Rao [48] proposed that specific soluble binding sites for these drugs, collectively termed peroxisome proliferators (PPs), were present in liver and kidney cell extracts [49, 50]. The PPAR gene was first cloned as a member of the steroid hormone receptor superfamily from a *m*-hepatic cDNA library [51]. This gene corresponds to PPARα, according to the current nomenclature. Two years later, three closely related members of the PPAR family (xPPARα, β, and γ) were isolated from a *Xenopus* ovary cDNA library and were shown to activate the promoter of the acyl coenzyme A oxidase (ACO) gene, which encodes the key peroxisomal fatty acid β-oxidation enzyme [52]. xPPARα is homologous to Issemann's PPARα [51], and xPPARγ is currently placed in the PPARγsubfamily, together with other homologous members found in mammals. Mammalian PPARδ was in a new PPAR group because of a difference in amino acid sequence compared with xPPARβ; however, it is presently considered to be a PPARβ and is designated as PPARβ/δ [45]. Of the three PPARs, PPARα is the most critical in the present review, because it is expressed at high levels in the liver, activates fatty acid catabolism, stimulates gluconeogenesis and ketone body synthesis, and participates in the control of lipoprotein assembly [45].

8.2. Species Differences in PPARα-Associated Signaling. The PPARα isotype has prime importance for studies with animal models to predict the effects of hepatic PPs in humans, because PPARα agonists induce seemingly quite different actions in rodents and humans [53]. Originally, as the name indicates, PPARs were studied because of their ability to bind PPs and consequently induce PP-metabolizing enzymes. In rats and mice, but not in humans, PPs such as hypolipidemic drugs, industrial plasticizers, and herbicides are non-genotoxic carcinogens that cause liver tumors [54]. In humans, these drugs function to maintain lipid homeostasis and do not induce peroxisome proliferation. Thus, the toxicity and carcinogenicity of PPs are highly species specific [55]. The species differences may be attributable to lower PPAR mRNA expression levels in *h*-hepatocytes compared with rodent cells [56, 57]. Alternatively, or additionally, species differences may be the result of different sensitivities of the genes associated with the peroxisome proliferation response to low levels of PPs, owing to structural differences in PPARα [54]. There are both similarities and differences in responses to xenobiotics among not only different species (interspecies) but also individuals of the same species (intraspecies). Interspecific PPARα diversity between rodents and humans is well known and has been studied with respect to drug metabolism. NR subfamily 1 members have at least two functions in mammals. One is to regulate peroxisome proliferation through binding to PPAR response elements (PPREs) in the promoters of genes such as ACO [58, 59], bifunctional dehydrogenase/hydratase (BFE) [60], and microsomal CYP4A1 [61]. The other is to modulate the serum cholesterol level by targeting genes such as the lipoprotein lipase gene [62] and the apolipoprotein regulating genes AI, AII, and CII [63]. The former mechanism appears to function in rodents, but not in humans, and is responsible for the induction of peroxisome proliferation and hepatocarcinogenesis, whereas the latter mechanism controls basic lipid metabolism in both rodents and humans [56]. This species difference in xenobiotic receptor/ligand signaling may be attributable to differences in the expression level of a receptor, or to differences in receptor/ligand binding affinity, and causes difficulty in determining responses in humans based on rodent data [56].

8.3. PPARα Gene-Humanized Mice. One approach to overcoming species differences is to generate "humanized" transgenic mice (gene-humanized mice), in which a *h*-gene of interest is introduced into the *m*-genome [17]. A PPARα gene-humanized *m*-line that expresses the *h*-PPARα gene [64] under the control of the tetracycline responsive regulatory system in the liver of murine PPARα gene-null mice [65] has been created. These mice functionally responded to the expected ligands as wild-type mice, but did not exhibit the hepatocellular proliferation, including increases in peroxisomes, seen in wild-type mice. Thus, this approach may help overcome species differences and provide animal models suitable for studying *h*-responses regulated by genes of interest.

8.4. PPAR Signaling in Chimeric Mice. Considering the prominent roles and the species divergence of PPARs in the response to xenobiotics, it is important to study *h*-PPAR-related responses of the *h/m*-chimeric mouse. We examined the effects of fibrates (antihyperlipidemic drugs and PPAR agonists) [63, 66] in the chimeric mice. Given the central role of the liver in PPAR-regulated lipid metabolism and the use of fibrate compounds in a variety of clinical drugs, the responses of *h/m*-chimeric mice to fibrates and PPARs may have important practical implications.

Hepatocytes secrete biliary phospholipids, composed largely of phosphatidylcholine (PC), through multidrug-resistance 2 P-glycoprotein (MDR3, or ABCB4) embedded in the canalicular membrane. MDR3 was shown to translocate PC in a study using mdr2 gene (a murine homolog of *h*-MDR3) knockout mice. These mice completely lack phospholipids in their bile [67], but the bile PC is fully recovered with the overexpression of *h*-MDR3 [68]. The expression level of the *h*-MDR3 gene affects the development of hepatobiliary diseases [69].

Fibrates upregulate mdr2 gene expression [70], which is associated with an increase in biliary phospholipid secretion [71]. Benzafibrate (BF), a second-generation fibrate analog, was clinically shown to reduce elevated serum biliary enzyme levels in patients with chronic cholestatic liver disease

[72]. It was shown to bind to PPARβ/δ and α, with a higher affinity for the former, and was thus said to be a bona fide PPAR ligand [73]. Other researchers created a coactivator-dependent receptor-ligand in vitro interaction assay and demonstrated that BF was a ligand for PPARα, β/δ, and γ [74]. The same researchers also showed drug-induced activation of PPARα/RXRα, PPARβ/δ/RXRα, and PPARγ/RXRα [74].

BF induces an increase in ABCB4 (MDR3), and its redistribution in the cell membrane. This induction was associated with an enhanced capacity of *h*-hepatocytes to direct PC into bile canaliculi [75]. Furthermore, ABCB4 redistribution was attenuated when PPARα expression was suppressed by small interfering RNA or morpholino antisense oligonucleotides in cultured HepG2 cells (hepatoblastoma cells) [75], strongly suggesting the necessity for PPARα in the BF-induced activation of PC secretion in *h*-hepatocytes.

We tested the ability of the *h/m*-chimeric *m*-liver to exhibit *h*-type PPAR-dependent responses by administering BF to the chimeric mice. Mice with RIs of 60–80% were fed a standard laboratory chow containing 0.3% (wt/wt) BF for 7 days, and their livers were analyzed for MDR3 mRNA and protein expression [39]. The mRNA level in the BF-treated mice was approximately 2-fold the level in non-treated control mice. The protein level was approximately 3.5-fold that in the controls. The fibrate induced a robust redistribution (exocytosis and insertion) of MDR3 proteins into the bile canaliculi.

Although studies on the expression and function of PPARs in the *h/m*-chimeric *m*-liver are limited, we conclude, based on the studies described above, that the chimeric *m*-liver exhibits the phenotypes of PPAR-regulated physiological and pathological processes, including responses to xenobiotics, that are normally present in the *h*-liver in vivo.

9. Summary and Prospective

After administration, a xenobiotic is generally and largely absorbed by the liver, intracellularly distributed, metabolized, and secreted through the bile or urinary ducts. These steps, collectively termed absorption, distribution, metabolism, and excretion (ADME), are interdependent, and drug pharmacokinetics are determined by the parameters resulting from these interactive processes. There are marked species differences in the many genes and proteins associated with ADME of a xenobiotic. The differences between humans and rodents dictate that pharmacokinetic data determined in rodents must be very cautiously, deliberately, and correctly extrapolated to humans in order to ensure that the drug will be safe and effective in patients. Until recently, *h*-hepatocyte-chimeric mice have been studied primarily in relation to CYP-associated metabolism, representing the M of ADME, and HCV/HBV infection. These studies have shown that the chimeric mice are significantly and appreciably humanized, providing a reliable and promising animal model for predicting drug metabolism and efficacy in humans. Although data have also been accumulated for the A, D, and E steps of ADME, more work is required before reaching an appropriate conclusion concerning the humanization of a chimeric mouse with respect to these processes. Nevertheless, currently available data appear to demonstrate that these processes are also well humanized.

Based on our studies and experiences to date, the *h*-hepatocyte-chimeric mice exhibit *h*-type liver responses at the gene and protein levels. These mice can mimic the steady-state expression in the *h*-liver in the absence of exogenous stimuli and exhibit the expected *h*-type responses upon stimulation. However, we must consider the limitations of chimeric mice. Current chimeric mice carry hepatocytes only of human origin, but all other cells are of *m*-origin. To perform liver functions, parenchymal cells require non-parenchymal cells, which are of mouse, and not of human, origin in the chimeric mice. Some interactions between *h*-hepatocytes and *m*-nonparenchymal cells may proceed as normal homogeneous interactions, and some may not.

In addition, endocrinological regulation is crucial for hepatocytes to achieve normal metabolic homeostasis and to return to normal conditions after endogenous or exogenous factors have caused metabolic parameters to extend beyond the normal range. Chimeric livers are under the influence of the *m*-endocrinological system, and some *m*-hormones such as growth hormone (GH) are not able to act on *h*-cells, because a hormone-receptor complex does not form between *m*-GH and *h*-hepatocyte receptors [76]. In support of this notion, *h*-hepatocytes administered with *h*-GH showed enhanced expression of liver growth-associated *h*-genes, including IGF-1, STAT-3, Cdc 25A, and cyclinD1, and repopulated the host liver at a rate approximately 6-fold that in the control. Despite these possible limitations, we consider the chimeric mouse to be the best animal model to date for *h*-liver function studies, because the chimeric mice with high RI values not only expressed *h*-liver proteins but also mimicked *h*-liver functions. Five years ago, we started mass production of homogenous populations of the hepatocyte-humanized mice with high RIs to facilitate research activities in the academic and industrial communities, including examinations of *h*-type metabolism of new drugs for *h*-use, the study of *h*-HCV infection mechanism and propagation, and the development of new anti-HCV-drugs. However, we are still in the initial stages of characterizing various aspects of the chimeric mice. Further study will systematically reveal the advantages and limits of this newly developed hepatocyte-humanized mouse.

Acknowledgments

The authors are grateful to Dr. Hardwich for the kind invitation to review the current status of the studies on chimeric mice, with an emphasis on PPAR signaling, as this will be an important issue in the utilization of chimeric mice for drug development. We thank Drs. T. Yokoi, T. Horie, and T. Inoue for kindly providing information related to PPAR-associated drug metabolism; Ms. T. Shimizu for assistance in preparing the manuscript; and Dr. A. Miyajima for kindly permitting us to present Figure 1 in our review.

We are much obliged to a recent review [1] on historical and histological aspects of chimeric mice, some parts of which are cited herein, and to an excellent review [17] that presented information on recent progress in xenobiotic metabolism studies, especially those using gene-engineered humanized mice to evaluate *h*-type xenobiotic metabolism. Our study of chimeric mice with livers composed of *h*-hepatocytes was supported by three programs, the Yoshizato project, Cooperative Link of Unique Science and Technology for Economy Revitalization (CLUSTER), Japanese Ministry of Education, Culture, Sports, Science, and Technology, the Hiroshima Prefecture to K. Yoshizato, Hiroshima University 21st Century COE Program for Advanced Radiation Casualty Medicine to K. Kamiya, and Advanced Medical Technology, Health, and Labor Sciences Research Grant from the Ministry of Health, Labor, and Welfare of Japan to T. Yokoi.

References

[1] K. Yoshizato, C. Tateno, and R. Utoh, "A human hepatocytes-bearing mouse: a novel animal model to study the mechanism of liver size control in mammals," *International Journal of Design & Nature*, vol. 4, no. 2, pp. 1–20, 2009.

[2] K. Nakatani, H. Okuyama, Y. Shimahara, et al., "Cytoglobin/STAP, its unique localization in splanchnic fibroblast-like cells and function in organ fibrogenesis," *Laboratory Investigation*, vol. 84, no. 1, pp. 91–101, 2004.

[3] F. Lemaigre and K. S. Zaret, "Liver development update: new embryo models, cell lineage control, and morphogenesis," *Current Opinion in Genetics & Development*, vol. 14, no. 5, pp. 582–590, 2004.

[4] G. K. Michalopoulos, "Liver regeneration," *Journal of Cellular Physiology*, vol. 213, no. 2, pp. 286–300, 2007.

[5] J. A. Rhim, E. P. Sandgren, R. D. Palmiter, and R. L. Brinster, "Complete reconstitution of mouse liver with xenogeneic hepatocytes," *Proceedings of the National Academy of Sciences of the United States of America*, vol. 92, no. 11, pp. 4942–4946, 1995.

[6] M. Dandri, M. R. Burda, E. Török, et al., "Repopulation of mouse liver with human hepatocytes and in vivo infection with hepatitis B virus," *Hepatology*, vol. 33, no. 4, pp. 981–988, 2001.

[7] D. F. Mercer, D. E. Schiller, J. F. Elliott, et al., "Hepatitis C virus replication in mice with chimeric human livers," *Nature Medicine*, vol. 7, no. 8, pp. 927–933, 2001.

[8] C. Tateno, Y. Yoshizane, N. Saito, et al., "Near completely humanized liver in mice shows human-type metabolic responses to drugs," *American Journal of Pathology*, vol. 165, no. 3, pp. 901–912, 2004.

[9] P. Meuleman, L. Libbrecht, R. De Vos, et al., "Morphological and biochemical characterization of a human liver in a uPA-SCID mouse chimera," *Hepatology*, vol. 41, no. 4, pp. 847–856, 2005.

[10] N. M. Kneteman and D. F. Mercer, "Mice with chimeric human livers: who says supermodels have to be tall?" *Hepatology*, vol. 41, no. 4, pp. 703–706, 2005.

[11] M. Nishimura, T. Yokoi, C. Tateno, et al., "Induction of human CYP1A2 and CYP3A4 in primary culture of hepatocytes from chimeric mice with humanized liver," *Drug Metabolism and Pharmacokinetics*, vol. 20, no. 2, pp. 121–126, 2005.

[12] J. L. Heckel, E. P. Sandgren, J. L. Degen, R. D. Palmiter, and R. L. Brinster, "Neonatal bleeding in transgenic mice expressing urokinase-type plasminogen activator," *Cell*, vol. 62, no. 3, pp. 447–456, 1990.

[13] E. P. Sandgren, R. D. Palmiter, J. L. Heckel, C. C. Daughterly, R. L. Brinster, and J. L. Degen, "Complete hepatic regeneration after somatic deletion of an albumin-plasminogen activator transgene," *Cell*, vol. 66, no. 2, pp. 245–256, 1991.

[14] J. A. Rhim, E. P. Sandgren, J. L. Degen, R. D. Palmiter, and R. L. Brinster, "Replacement of diseased mouse liver by hepatic cell transplantation," *Science*, vol. 263, no. 5150, pp. 1149–1152, 1994.

[15] N. Kawada, D. B. Kristensen, K. Asahina, et al., "Characterization of a stellate cell activation-associated protein (STAP) with peroxidase activity found in rat hepatic stellate cells," *The Journal of Biological Chemistry*, vol. 276, no. 27, pp. 25318–25323, 2001.

[16] M. Nishimura, H. Yoshitsugu, T. Yokoi, et al., "Evaluation of mRNA expression of human drug-metabolizing enzymes and transporters in chimeric mouse with humanized liver," *Xenobiotica*, vol. 35, no. 9, pp. 877–890, 2005.

[17] F. J. Gonzalez and A.-M. Yu, "Cytochrome P450 and xenobiotic receptor humanized mice," *Annual Review of Pharmacology and Toxicology*, vol. 46, pp. 41–64, 2006.

[18] N. J. Hewitt, E. L. Lecluyse, and S. S. Ferguson, "Induction of hepatic cytochrome P450 enzymes: methods, mechanisms, recommendations, and in vitro-in vivo correlations," *Xenobiotica*, vol. 37, no. 10-11, pp. 1196–1224, 2007.

[19] M. J. Graham and B. G. Lake, "Induction of drug metabolism: species differences and toxicological relevance," *Toxicology*, vol. 254, no. 3, pp. 184–191, 2008.

[20] J. J. P. Bogaards, M. Bertrand, P. Jackson, et al., "Determining the best animal model for human cytochrome P450 activities: a comparison of mouse, rat, rabbit, dog, micropig, monkey and man," *Xenobiotica*, vol. 30, no. 12, pp. 1131–1152, 2000.

[21] J. Caldwell, "The current status of attempts to predict species differences in drug metabolism," *Drug Metabolism Reviews*, vol. 12, no. 2, pp. 221–237, 1981.

[22] U. M. Zanger, S. Raimundo, and M. Eichelbaum, "Cytochrome P450 2D6: overview and update on pharmacology, genetics, biochemistry," *Naunyn-Schmiedeberg's Archives of Pharmacology*, vol. 369, no. 1, pp. 23–37, 2004.

[23] A.-M. Yu, J. R. Idle, and F. J. Gonzalez, "Polymorphic cytochrome P450, 2D6: humanized mouse model and endogenous substrates," *Drug Metabolism Reviews*, vol. 36, no. 2, pp. 243–277, 2004.

[24] Y. Masubuchi, T. Iwasa, S. Hosokawa, et al., "Selective deficiency of debrisoquine 4-hydroxylase activity in mouse liver microsomes," *Journal of Pharmacology and Experimental Therapeutics*, vol. 282, no. 3, pp. 1435–1441, 1997.

[25] M. Katoh, T. Sawada, Y. Soeno, et al., "In vivo drug metabolism model for human cytochrome P450 enzyme using chimeric mice with humanized liver," *Journal of Pharmaceutical Sciences*, vol. 96, no. 2, pp. 428–437, 2007.

[26] W. P. Bowen, J. E. Carey, A. Miah, et al., "Measurement of cytochrome P450 gene induction in human hepatocytes, using quantitative real-time reverse transcriptase-polymerase chain reaction," *Drug Metabolism and Disposition*, vol. 28, no. 7, pp. 781–788, 2000.

[27] M. Katoh, T. Matsui, M. Nakajima, et al., "In vivo induction of human cytochrome P450 enzymes expressed in chimeric mice with humanized liver," *Drug Metabolism and Disposition*, vol. 33, no. 6, pp. 754–763, 2005.

[28] T. Toriyabe, K. Nagata, T. Takada, et al., "Unveiling a new essential cis element for the transactivation of the CYP3A4

gene by xenobiotics," *Molecular Pharmacology*, vol. 75, no. 3, pp. 677–684, 2009.

[29] S. A. Jones, L. B. Moore, J. L. Shenk, et al., "The pregnane X receptor: a promiscuous xenobiotic receptor that has diverged during evolution," *Molecular Endocrinology*, vol. 14, no. 1, pp. 27–39, 2000.

[30] I. J. Cho and S. G. Kim, "Oltipraz inhibits 3-methylcholanthrene induction of CYP1A1 by CCAAT/enhancer-binding protein activation," *The Journal of Biological Chemistry*, vol. 278, no. 45, pp. 44103–44112, 2003.

[31] T. D. Bjornsson, J. T. Callaghan, H. J. Einolf, et al., "The conduct of in vitro and in vivo drug-drug interaction studies: a Pharmaceutical Research and Manufacturers of America (PhRMA) perspective," *Drug Metabolism and Disposition*, vol. 31, no. 7, pp. 815–832, 2003.

[32] M. Katoh, T. Matsui, H. Okumura, et al., "Expression of human phase II enzymes in chimeric mice with humanized liver," *Drug Metabolism and Disposition*, vol. 33, no. 9, pp. 1333–1340, 2005.

[33] W. Xie, M.-F. Yeuh, A. Radominska-Pandya, et al., "Control of steroid, heme, and carcinogen metabolism by nuclear pregnane X receptor and constitutive androstane receptor," *Proceedings of the National Academy of Sciences of the United States of America*, vol. 100, no. 7, pp. 4150–4155, 2003.

[34] S. Kodama, C. Koike, M. Negishi, and Y. Yamamoto, "Nuclear receptors CAR and PXR cross talk with FOXO1 to regulate genes that encode drug-metabolizing and gluconeogenic enzymes," *Molecular and Cellular Biology*, vol. 24, no. 18, pp. 7931–7940, 2004.

[35] J. Zhang, W. Huang, S. S. Chua, P. Wei, and D. D. Moore, "Modulation of acetaminophen-induced hepatotoxicity by the xenobiotic receptor CAR," *Science*, vol. 298, no. 5592, pp. 422–424, 2002.

[36] H. Okumura, M. Katoh, T. Sawada, et al., "Humanization of excretory pathway in chimeric mice with humanized liver," *Toxicological Sciences*, vol. 97, no. 2, pp. 533–538, 2007.

[37] H. Ko, E. Novak, G. R. Peters, et al., "Pharmacokinetics of single-dose cefmetazole following intramuscular administration of cefmetazole sodium to healthy male volunteers," *Antimicrobial Agents and Chemotherapy*, vol. 33, no. 4, pp. 508–512, 1989.

[38] T. Murakawa, H. Sakamoto, S. Fukada, et al., "Pharmacokinetics of ceftizoxime in animals after parenteral dosing," *Antimicrobial Agents and Chemotherapy*, vol. 17, no. 2, pp. 157–164, 1980.

[39] J. Shoda, K. Okada, Y. Inada, et al., "Bezafibrate induces multidrug-resistance P-glycoprotein 3 expression in cultured human hepatocytes and humanized livers of chimeric mice," *Hepatology Research*, vol. 37, no. 7, pp. 548–556, 2007.

[40] S. A. Sarbah and Z. M. Younossi, "Hepatitis C: an update on the silent epidemic," *Journal of Clinical Gastroenterology*, vol. 30, no. 2, pp. 125–143, 2000.

[41] P. Meuleman and G. Leroux-Roels, "The human liver-uPA-SCID mouse: a model for the evaluation of antiviral compounds against HBV and HCV," *Antiviral Research*, vol. 80, no. 3, pp. 231–238, 2008.

[42] M. Tsuge, N. Hiraga, H. Takaishi, et al., "Infection of human hepatocyte chimeric mouse with genetically engineered hepatitis B virus," *Hepatology*, vol. 42, no. 5, pp. 1046–1054, 2005.

[43] Nuclear Receptors Nomenclature Committee, "A unified nomenclature system for the nuclear receptor superfamily," *Cell*, vol. 97, no. 2, pp. 161–163, 1999.

[44] S. Yu and J. K. Reddy, "Transcription coactivators for peroxisome proliferator-activated receptors," *Biochimica et Biophysica Acta*, vol. 1771, no. 8, pp. 936–951, 2007.

[45] L. Michalik, J. Auwerx, J. P. Berger, et al., "International union of pharmacology. LXI. Peroxisome proliferator-activated receptors," *Pharmacological Reviews*, vol. 58, no. 4, pp. 726–741, 2006.

[46] E. A. Lock, A. M. Mitchell, and C. R. Elcombe, "Biochemical mechanisms of induction of hepatic peroxisome proliferation," *Annual Review of Pharmacology and Toxicology*, vol. 29, pp. 145–163, 1989.

[47] M. R. Nemali, M. K. Reddy, N. Usuda, et al., "Differential induction and regulation of peroxisomal enzyme: predictive value of peroxisome proliferation in identifying certain non-mutagenic carcinogens," *Toxicology and Applied Pharmacology*, vol. 97, no. 1, pp. 72–87, 1989.

[48] J. K. Reddy and M. S. Rao, "Peroxisome proliterators and cancer: mechanisms and implications," *Trends in Pharmacological Sciences*, vol. 7, pp. 438–443, 1986.

[49] N. D. Lalwani, W. E. Fahl, and J. K. Reddy, "Detection of a nafenopin binding protein in rat liver cytosol associated with the induction of peroxisome proliferation by hypolipidemic compounds," *Biochemical and Biophysical Research Communications*, vol. 116, no. 2, pp. 388–393, 1983.

[50] S. Goldfischer and J. K. Reddy, "Peroxisomes (microbodies) in cell pathology," *International Review of Experimental Pathology*, vol. 26, pp. 45–84, 1984.

[51] I. Issemann and S. Green, "Activation of a member of the steroid hormone receptor superfamily by peroxisome proliferators," *Nature*, vol. 347, no. 6294, pp. 645–650, 1990.

[52] C. Dreyer, G. Krey, H. Keller, F. Givel, G. Helftenbein, and W. Wahli, "Control of the peroxisomal β-oxidation pathway by a novel family of nuclear hormone receptors," *Cell*, vol. 68, no. 5, pp. 879–887, 1992.

[53] K. Tachibana, D. Yamasaki, K. Ishimoto, and T. Doi, "The role of PPARs in cancer," *PPAR Research*, vol. 2008, Article ID 102737, 15 pages, 2008.

[54] K. Morimura, C. Cheung, J. M. Ward, J. K. Reddy, and F. J. Gonzalez, "Differential susceptibility of mice humanized for peroxisome proliferator-activated receptor α to Wy-14,643-induced liver tumorigenesis," *Carcinogenesis*, vol. 27, no. 5, pp. 1074–1080, 2006.

[55] P. Bentley, I. Calder, C. Elcombe, P. Grasso, D. Stringer, and H.-J. Wiegand, "Hepatic peroxisome proliferation in rodents and its significance for humans," *Food and Chemical Toxicology*, vol. 31, no. 11, pp. 857–907, 1993.

[56] P. R. Holden and J. D. Tugwood, "Peroxisome proliferator-activated receptor alpha: role in rodent liver cancer and species differences," *Journal of Molecular Endocrinology*, vol. 22, no. 1, pp. 1–8, 1999.

[57] C. N. A. Palmer, M.-H. Hsu, K. J. Griffin, J. L. Raucy, and E. F. Johnson, "Peroxisome proliferator activated receptor-α expression in human liver," *Molecular Pharmacology*, vol. 53, no. 1, pp. 14–22, 1998.

[58] J. D. Tugwood, I. Issemann, R. G. Anderson, K. R. Bundell, W. L. McPheat, and S. Green, "The mouse peroxisome proliferator activated receptor recognizes a response element in the 5′ flanking sequence of the rat acyl CoA oxidase gene," *The EMBO Journal*, vol. 11, no. 2, pp. 433–439, 1992.

[59] B. Zhang, S. L. Marcus, F. G. Saijadi, et al., "Identification of a peroxisome proliferator-responsive element upstream of the gene encoding rat peroxisomal enoyl-CoA hydratase/3-hydroxyacyl-CoA dehydrogenase," *Proceedings of the National*

Academy of Sciences of the United States of America, vol. 89, no. 16, pp. 7541–7545, 1992.

[60] O. Bardot, T. C. Aldridge, N. Latruffe, and S. Green, "PPAR-RXR heterodimer activates a peroxisome proliferator response element upstream of the bifunctional enzyme gene," *Biochemical and Biophysical Research Communications*, vol. 192, no. 1, pp. 37–45, 1993.

[61] T. C. Aldridge, J. D. Tugwood, and S. Green, "Identification and characterization of DNA elements implicated in the regulation of CYP4A1 transcription," *Biochemical Journal*, vol. 306, part 2, pp. 473–479, 1995.

[62] K. Schoonjans, J. Peinado-Onsurbe, A.-M. Lefebvre, et al., "PPARα and PPARγ activators direct a distinct tissue-specific transcriptional response via a PPRE in the lipoprotein lipase gene," *The EMBO Journal*, vol. 15, no. 19, pp. 5336–5348, 1996.

[63] J. M. Peters, N. Hennuyer, B. Staels, et al., "Alterations in lipoprotein metabolism in peroxisome proliferator-activated receptor α-deficient mice," *The Journal of Biological Chemistry*, vol. 272, no. 43, pp. 27307–27312, 1997.

[64] C. Cheung, T. E. Akiyama, J. M. Ward, et al., "Diminished hepatocellular proliferation in mice humanized for the nuclear receptor peroxisome proliferator-activated receptor α," *Cancer Research*, vol. 64, no. 11, pp. 3849–3854, 2004.

[65] S. S. Lee, T. Pineau, J. Drago, et al., "Targeted disruption of the α isoform of the peroxisome proliferator-activated receptor gene in mice results in abolishment of the pleiotropic effects of peroxisome proliferators," *Molecular and Cellular Biology*, vol. 15, no. 6, pp. 3012–3022, 1995.

[66] C.-H. Lee, P. Olson, and R. M. Evans, "Lipid metabolism, metabolic diseases, and peroxisome proliferator-activated receptors," *Endocrinology*, vol. 144, no. 6, pp. 2201–2207, 2003.

[67] J. J. M. Smit, A. H. Schinkel, R. P. J. Oude Elferink, et al., "Homozygous disruption of the murine *mdr2* P-glycoprotein gene leads to a complete absence of phospholipid from bile and to liver disease," *Cell*, vol. 75, no. 3, pp. 451–462, 1993.

[68] A. J. Smith, J. M. L. de Vree, R. Ottenhoff, R. P. J. Oude Elferink, A. H. Schinkel, and P. Borst, "Hepatocyte-specific expression of the human *MDR3* P-glycoprotein gene restores the biliary phosphatidylcholine excretion absent in *Mdr2* (-/-) mice," *Hepatology*, vol. 28, no. 2, pp. 530–536, 1998.

[69] O. Rosmorduc, B. Hermelin, P.-Y. Boelle, R. Parc, J. Taboury, and R. Poupon, "*ABCB4* gene mutation-associated cholelithiasis in adults," *Gastroenterology*, vol. 125, no. 2, pp. 452–459, 2003.

[70] T. Kok, V. W. Bloks, H. Wolters, et al., "Peroxisome proliferator-activated receptor α (PPARα)-mediated regulation of multidrug resistance 2 (Mdr2) expression and function in mice," *Biochemical Journal*, vol. 369, part 3, pp. 539–547, 2003.

[71] J. Chianale, V. Vollrath, A. M. Wielandt, et al., "Fibrates induce mdr2 gene expression and biliary phospholipid secretion in the mouse," *Biochemical Journal*, vol. 314, part 3, pp. 781–786, 1996.

[72] T. Kurihara, A. Niimi, A. Maeda, M. Shigemoto, and K. Yamashita, "Bezafibrate in the treatment of primary biliary cirrhosis: comparison with ursodeoxycholic acid," *American Journal of Gastroenterology*, vol. 95, no. 10, pp. 2990–2992, 2000.

[73] G. Krey, O. Braissant, F. L'Horset, et al., "Fatty acids, eicosanoids, and hypolipidemic agents identified as ligands of peroxisome proliferator-activated receptors by coactivator-dependent receptor ligand assay," *Molecular Endocrinology*, vol. 11, no. 6, pp. 779–791, 1997.

[74] I. Inoue, F. Itoh, S. Aoyagi, et al., "Fibrate and statin synergistically increase the transcriptional activities of PPARα/RXRα and decrease the transactivation of NFκB," *Biochemical and Biophysical Research Communications*, vol. 290, no. 1, pp. 131–139, 2002.

[75] J. Shoda, Y. Inada, A. Tsuji, et al., "Bezafibrate stimulates canalicular localization of NBD-labeled PC in HepG2 cells by PPARα-mediated redistribution of ABCB4," *Journal of Lipid Research*, vol. 45, no. 10, pp. 1813–1825, 2004.

[76] N. Masumoto, C. Tateno, A. Tachibana, et al., "GH enhances proliferation of human hepatocytes grafted into immunodeficient mice with damaged liver," *Journal of Endocrinology*, vol. 194, no. 3, pp. 529–537, 2007.

ELSEVIER

Journal of Hepatology 51 (2009) 1046–1054

Journal of Hepatology

www.elsevier.com/locate/jhep

Absence of viral interference and different susceptibility to interferon between hepatitis B virus and hepatitis C virus in human hepatocyte chimeric mice☆

Nobuhiko Hiraga[1,2], Michio Imamura[1,2], Tsuyoshi Hatakeyama[1], Shosuke Kitamura[1], Fukiko Mitsui[1,b], Shinji Tanaka[1], Masataka Tsuge[1,2], Shoichi Takahashi[1,2], Hiromi Abe[2,3], Toshiro Maekawa[2,3], Hidenori Ochi[2,3], Chise Tateno[2,4], Katsutoshi Yoshizato[2,4,5], Takaji Wakita[6], Kazuaki Chayama[1,2,3,*]

[1]*Department of Medicine and Molecular Science, Division of Frontier Medical Science, Programs for Biomedical Research, Graduate School of Biomedical Sciences, Hiroshima University, 1-2-3 Kasumi, Minami-ku, Hiroshima 734-8551, Japan*

[2]*Liver Research Project Center, Hiroshima University, Hiroshima, Japan*

[3]*Laboratory for Liver Diseases, SNP Research Center, The Institute of Physical and Chemical Research (RIKEN), Yokohama, Japan*

[4]*PhoenixBio Co., Ltd., Higashihiroshima, Japan*

[5]*Osaka City University Graduate School of Medicine, Osaka, Japan*

[6]*Department of Virology II, National Institute of Infectious Diseases, Shinjuku-ku, Japan*

Background/Aims: **Both hepatitis B virus (HBV) and hepatitis C virus (HCV) replicate in the liver and show resistance against innate immunity and interferon (IFN) treatment. Whether there is interference between these two viruses is still controversial. We investigated the interference between these two viruses and the mode of resistance against IFN.**

Methods: **We performed infection experiments with either or both of the two hepatitis viruses in human hepatocyte chimeric mice. Huh7 cell lines with stable production of HBV were also established and transfected with HCV JFH1 clone. Mice and cell lines were treated with IFN. The viral levels in mice sera and culture supernatants and messenger RNA levels of IFN-stimulated genes were measured.**

Results: **No apparent interference between the two viruses was seen *in vivo*. Only a small (0.3 log) reduction in serum HBV and a rapid reduction in HCV were observed after IFN treatment, regardless of infection with the other virus. In *in vitro* studies, no interference between the two viruses was observed. The effect of IFN on each virus was not affected by the presence of the other virus. IFN-induced reductions of viruses in culture supernatants were similar to those in *in vivo* study.**

Conclusions: **No interference between the two hepatitis viruses exists in the liver in the absence of hepatitis. The mechanisms of IFN resistance of the two viruses target different areas of the IFN system.**

Keywords: **Superinfection; JFH-1; IFN-stimulated genes**

Received 4 February 2009; received in revised form 14 July 2009; accepted 15 July 2009; available online 23 September 2009

Associate Editor: F. Zoulim

☆ C.T. and K.Y. are employees of PhoenixBio Co. Ltd., Higashihiroshima, Japan. The other authors who have taken part in this study declared that they do not have anything to disclose regarding funding from industry or conflict of interest with respect to this manuscript.

* Corresponding author. Tel.: +81 82 2575190; fax: +81 82 2556220.

E-mail address: chayama@hiroshima-u.ac.jp (K. Chayama).

Abbreviations: GAPDH, glyceraldehydes-3-phosphate dehydrogenase; HBeAg, hepatitis B e antigen; HBsAg, hepatitis B surface antigen; HBV, hepatitis B virus; HCV, hepatitis C virus; IFN, interferon; OAS, 2′,5′-oligoadenylate synthetase; PCR, polymerase chain reaction; SCID, severe combined immunodeficiency; uPA, urokinase-type plasminogen activator.

0168-8278/$36.00
doi:10.1016/j.jhep.2009.09.002

1. Introduction

Both hepatitis B virus (HBV) and hepatitis C virus (HCV) infections are serious health problems worldwide. More than 350 million people are infected with HBV, and more than 170 million people are infected with HCV [1,2]. Both types of hepatitis viruses result in the development of chronic liver infection and lead to death due to liver failure and hepatocellular carcinoma [3]. To date, interferon (IFN) remains one of the most important drugs available for the treatment of both types of hepatitis viral infections. Although it is assumed that IFN suppresses viral replication through the effect of IFN-induced gene products such as mixovirus resistance protein A (MxA), RNA-dependent protein kinase (PKR), and 2′,5′-oligoadenylate synthetase (OAS) [4], the precise mechanism of action of these proteins on both hepatitis viruses are unknown.

Coinfection with both viruses leads to a rapid and severe progression of chronic liver disease [5], with a higher risk of hepatocellular carcinoma [6]. Currently, there is a debate about whether or not there is interference between the two hepatitis viruses, with some favoring such interference [7] and others arguing against such a concept [8]. A number of mechanisms can cause interference between viruses. A major mechanism of interference is induction of IFN by one virus to prevent replication of the second virus; however, viruses develop their own strategies to resist the effect of IFN. In clinical practice, practitioners often perceive that reduction of HBV in serum by IFN therapy is poorer compared with HCV. HCV levels in sera of IFN-treated patients decrease relatively rapidly, and a proportion of patients eventually show complete eradication of the virus. Furthermore, the recent use of pegylated IFN (PEG-IFN) in combination with ribavirin has improved the eradication rate [9]. Eradication of HBV by IFN, however, is usually difficult, even when using IFN combined with ribavirin [10].

The mechanisms developed by viruses to resist host innate immunity, including IFN signaling, are well established in some viruses. Such mechanisms involve interruption of IFN signaling by interacting molecules that transduce the signal from the IFN receptor through the Janus kinase (Jak) signal transducer and activator of transcription (STAT) pathway [4]. Viral proteins of paramixoviruses, for example, inhibit IFN signaling [11]. Several studies have also examined the mechanisms by which HCV resists the host immune system. These include degradation of Cardif adaptor protein by NS3A/4 protease [12]. Generally, expression of HCV protein is associated with inhibition of STAT1 function independent of STAT tyrosine phosphorylation [13]. Additionally, expression of the HCV core protein in cultured cells is associated with increased expression levels of the suppressor of cytokine signaling 3 (SOCS-3) [14]. The NS5A and E2 proteins are both inhibitors of PKR [15]. These strong actions of HCV against innate immunity are consistent with the high chronicity rate of the virus. IFN, however, effectively reduces HCV replicon in Huh7 cells [16], suggesting that the virus has little potential to disturb the actions of IFN.

In contrast to HCV, the mechanisms of IFN resistance by HBV are poorly understood. To date, only a few studies have reported the molecular mechanisms of HBV resistance against the actions of IFN. The HBV-related resistance to IFN, for example, involves upregulation of protein phosphatase 2A (PP2A) as the primary event, which subsequently leads to inhibition of protein arginine methyltransferase 1 (PRMT1) and reduced STAT1 methylation [17]. In addition to these molecular mechanisms, microarray analyses of serial liver biopsies of experimentally infected chimpanzees showed striking differences in the early immune responses to HBV and HCV. HCV, for example, induced early changes in the expression of many intrahepatic genes, including genes involved in type 1 IFN response [18], whereas HBV did not induce any detectable changes in the expression of intrahepatic genes in the first weeks of infection [19].

HBV–HCV double infection is a good model to use for assessment of the mechanism of IFN resistance by these two viruses because one can test the effect of IFN on one virus in the presence of the other virus. Recently, Bellecave et al. [20] established a novel *in vitro* model system in Huh7 cells that allowed the analysis of both viruses in a replicating context and reported the absence of direct viral interference. To this end, we used human hepatocyte chimeric mice and cell culture systems in the present study. The results showed that the presence of HBV does not affect the actions of IFN on HCV and vice versa. These results suggest the lack of interference between the two viruses in liver cells and indicate that the reported interference between the two viruses might be via inflammation including death of infected cells by cytotoxic T cells, cytokines including IFN-α and IFN-β, and interleukins produced by hepatocytes and infiltrating T cells.

2. Materials and methods

2.1. Transfection of Huh7 cells with HBV DNA and HCV RNA

Huh7 cells were grown in Dulbecco's modified Eagle's medium supplemented with 10% (v/v) fetal bovine serum at 37 °C and under 5% CO_2. Cloning of HBV DNA and the plasmid construction were performed as described previously [21]. For production of stably transfected cell lines, Huh7 cells were seeded onto 90-mm-diameter culture dishes. Twenty micrograms of the plasmid pTRE-HB-wt [21] was transfected by the calcium phosphate precipitation method. Twenty-four hours after transfection, the cells were split and cultured in Hygromycin B-DMEM selection medium (300 μg/ml; Invitrogen Japan K.K., Osaka, Japan), while 50 colonies were isolated and cultured for identification of virus-producing cell lines. Clones positive

for both hepatitis B surface antigen (HBsAg) and hepatitis B e antigen (HBeAg) were selected and further analyzed for production of HBV particles. Finally, three cell lines that produced more than 10^5 copies per milliliter of HBV DNA in supernatant were selected and used for further experiments.

For transfection with HCV RNA, we used pJFH1, which contains the complementary DNA of full-length genotype 2a HCV clone JFH1 downstream of the T7 promoter [22]. *In vitro* synthesis of HCV RNA and electroporation into Huh7 cells were performed as described previously [22,23]. Briefly, cells were treated with trypsin, washed twice with ice-cold RNase-free phosphate-buffered saline, and resuspended in Opti-MEM I (Invitrogen, Carlsbad, CA, USA) at a final concentration of 7.5×10^6 cells per milliliter. Then, 10 μg of HCV RNA to be electroporated was mixed with 0.4 mL of cell suspension and subjected to an electric pulse (950 μF and 260 V) using the Gene Pulser II Electroporation System (Bio-Rad, Hercules, CA, USA). After electroporation, the cell suspension was left for 5 min at room temperature and then incubated under normal culture conditions in a 10-cm-diameter cell culture dish.

2.2. Generation of human hepatocyte chimeric mice

Generation of the urokinase-type plasminogen activator $(uPA)^{+/+}$ and severe combined immunodeficiency $(SCID)^{+/+}$ mice and transplantation of human hepatocytes were performed as described recently by our group [21,23,24]. All mice were transplanted with frozen human hepatocytes obtained from the same donor. Infection, extraction of serum samples, and euthanasia were performed under ether anesthesia. The concentration of serum human serum albumin, which correlates with the repopulation index [24], was measured in mice as described previously [21]. All animal protocols described in this study were performed in accordance with the guidelines of the local committee for animal experiments. The experimental protocol was approved by the Ethics Review Committee for Animal Experimentation of Graduate School of Biomedical Sciences, Hiroshima University, Hiroshima, Japan.

2.3. Human serum samples

Human serum samples containing high titers of either HBV DNA (5.3×10^6 copies per milliliter) or genotype 1b HCV (2.2×10^6 copies per milliliter) were obtained from patients with chronic hepatitis with a written informed consent. The individual serum samples were divided into small aliquots and separately stored in liquid nitrogen until use. Chimeric mice were injected intravenously with 50 μL of either HBV- or HCV-positive human serum. Some mice were injected with HBV-positive human serum at 6 weeks after injection of HCV-positive human serum.

2.4. Analysis of HBV and HCV

HBsAg and HBeAg in culture supernatants were measured by commercially available enzyme-linked immunosorbent assay (ELISA) kits (Abbott Japan, Osaka, Japan). DNA was extracted from these samples by SMITEST (Genome Science Laboratories, Tokyo, Japan) and dissolved in 20 μL H_2O [21,25]. RNA was extracted from serum samples by Sepa Gene RV-R (Sankojunyaku, Tokyo), dissolved in 8.8 μL RNase-free H_2O, and reverse transcribed using random primer (Takara Bio Inc., Shiga, Japan) and M-MLV reverse transcriptase (ReverTra Ace, TOYOBO Co., Osaka, Japan) in a 20-μL reaction mixture according to the instructions provided by the manufacturer [23]. HCV core antigen in the culture medium was detected with HCV Ag assay (Ortho-Clinical Diagnostics, Rochester, NY, USA).

2.5. RNA extraction and measurement of mRNAs of interferon-induced genes by quantitative reverse transcription-polymerase chain reaction

Total RNA was extracted from cell lines using the RNeasy Mini Kit (Qiagen, Valencia, CA, USA). One nanogram of each RNA was reverse transcribed with ReverseTra Ace (TOYOBO Co.) and Random Primer (Takara Bio, Kyoto, Japan). We quantified the transcripts for MxA, OAS, and PKR. Amplification and detection were performed using ABI PRISM 7300 (Applied Biosystems, Foster City, CA, USA). Results were normalized to the transcript levels of glyceraldehydes-3-phosphate dehydrogenase (GAPDH).

2.6. Statistical analysis

Changes in HBV DNA and HCV RNA in mice sera were compared by Mann–Whitney test and unpaired *t* test. Differences in HBV DNA and HCV core antigen in mice sera and culture supernatants were analyzed by one-way analysis of variance followed by Scheffe's test. A P value of <0.05 was considered statistically significant.

3. Results

3.1. Infection of chimeric mouse with HBV and HCV and susceptibility to interferon

To investigate the interference between HBV and HCV and to examine the effect of IFN on both of these two viruses *in vivo*, we used six human chimeric mice. Each of six mice was inoculated intravenously with 50 μL of serum samples obtained from either HBV- or HCV-positive patients. The median HBV DNA level in HBV-positive serum-inoculated mice was 1.4×10^8 copies per milliliter (range: 5.3×10^6–3.6×10^9 copies per milliliter) at 6 weeks after inoculation (Fig. 1A), similar to our recent observation [21]. Similarly, the median HCV RNA level in HCV-positive human serum-inoculated mice was 1.0×10^7 copies per milliliter (range: 1.2×10^6–0.8×10^7 copies per milliliter) at 4 weeks after inoculation (Fig. 1B), as reported recently by our group [23]. Six weeks after inoculation, three of six HBV- or HCV-infected mice were treated daily with 7000 IU/g per day of intramuscular IFN-α for 2 weeks. Treatment resulted in a decrease of only 0.3 log in mice serum HBV DNA level compared to that in mice without treatment (Fig. 1A). In contrast, the same therapy resulted in a rapid decrease in HCV RNA to undetectable levels, as confirmed by quantitative polymerase chain reaction (PCR; Fig 1B).

To investigate the direct interference of the two viruses, we performed double-infection experiments. Ten chimeric mice were first inoculated intravenously with 50 μL of HCV-positive human serum samples. Six weeks after HCV infection when the mice developed HCV viremia, 50 μL of HBV-positive human serum samples were inoculated intravenously in 5 of 10 HCV-infected mice. All five mice became positive for both HBV and HCV at 2 weeks after HBV infection. No significant decrease in HCV RNA levels was observed in these superinfected mice before or after the development of HBV viremia (Fig. 2A). After HBV infection, there was no apparent decrease in HCV titer (Fig. 2B). Moreover, HBV DNA level in HBV–HCV-coinfected mice was comparable with that of only HBV-infected mice (Fig. 2B). These results sug-

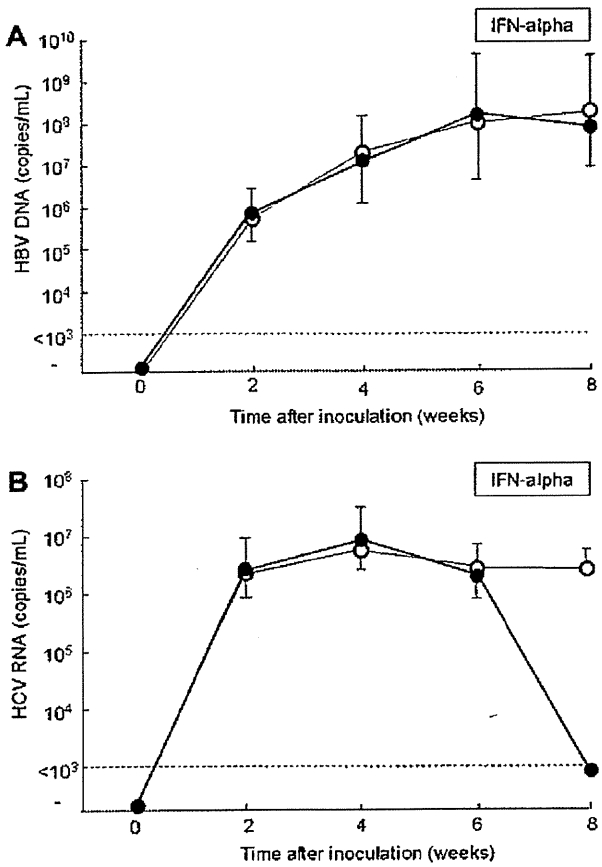

Fig. 1. Changes in serum virus titers in mice inoculated with hepatitis B virus (HBV) – positive or hepatitis C virus (HCV) – positive human serum samples. (A) HBV DNA levels in six mice inoculated with HBV-positive serum samples. (B) HCV RNA levels in six mice inoculated with HCV-positive serum samples. Six weeks after inoculation, three of six mice were treated daily with (closed circles) or without (open circles) 7000 IU/g per day of interferon-alpha intramuscularly for 2 weeks. Mice serum samples were extracted every 2 weeks after inoculation. Data are mean plus or minus standard deviation ($n = 3$). The horizontal dashed line represents the detection limit (10^3 copies per milliliter).

gest no interference between the two viruses in mice, which lack immunocytes known to cause hepatitis.

To further investigate if infection with either of the two hepatitis viruses alters the effect of IFN against the other virus, three HBV–HCV-coinfected mice were treated with IFN-α (Fig. 3A). Such treatment resulted in a rapid decrease in HCV RNA in all mice to undetectable levels as confirmed by quantitative PCR (Fig. 3B). In contrast, no significant decrease in HBV DNA titers was observed in these mice (Fig. 3B). These results are similar to the reduction of HCV RNA and HBV DNA in mice that were infected with either of these hepatitis viruses. These results indicate that HCV is more susceptible to IFN-α than HBV and that each virus does not alter the effect of IFN on the other virus. Because the effect of IFN on HCV was not disturbed by HBV, we assumed that HBV has no effect on the signal from IFN receptor to IFN-stimulated genes. It is possible, however, that HBV and HCV replicated in different cells in these mice. Because it was impossible to detect HCV protein and RNA in HCV-infected mouse liver by histologic examination, we performed *in vitro* experiments.

3.2. Production of both HBV- and HCV-producing cells and the effect of interferon

To investigate the effect of IFN on HBV and HCV *in vitro*, we created cell lines that produce both HBV and HCV. First, we established stable HBV-producing Huh7 cell lines. Three cell lines (Clone-39, -42, and -53) that produced HBsAg, HBeAg, and HBV DNA into the supernatant were selected (Table 1). These cell lines continuously produced HBV for more than 3 months (data not shown). Next, JFH1 RNA was transfected into these HBV-producing cell lines to produce both HBV DNA and HCV proteins into the supernatant. HBV DNA levels in the supernatants of these cell lines decreased in Clone-39, increased in Clone-42, and did not change in Clone-53 after JFH1 transfection (Fig. 4A). In contrast, HCV core antigen levels in the supernatants were higher in two of the three cell lines (Clone-39 and -42) than in Huh7 cells, and the level was not different in the remaining cell line (Clone-53) (Fig. 4B). These results indicate that the production of each of the two viruses does not disturb the replication of the other virus.

3.3. Effects of interferon on HBV and HCV in vitro

The effects of IFN on virus production in both HBV- and HCV-producing cell lines was examined by adding different amounts of IFN-α (0, 50, and 500 IU/mL) into the culture. The mRNA levels of intracellular IFN-stimulated genes such as MxA, OAS, and PKR increased in a dose-dependent manner in all three cell lines as well as in parental Huh7 cells (Fig. 5A). Following the addition of IFN, no apparent reduction of HBV was noted in the supernatant of HBV–HCV-cotransfected cell lines (Fig. 5B). In contrast, the levels of HCV core antigen in the supernatant decreased in all three cell lines treated with IFN, and the decrease was dose-dependent (Fig. 5C).

4. Discussion

Although IFN treatment for chronic HCV infection has improved with the advent of PEG-IFN, the rate of viral eradication remains unsatisfactory [9]. The mechanism responsible for failure of IFN to eradicate the virus completely must be clarified. To study the mechanism of viral resistance against IFN, analysis of viral interference may give us some hints because one of the major mechanisms of interference is through the action of IFN.

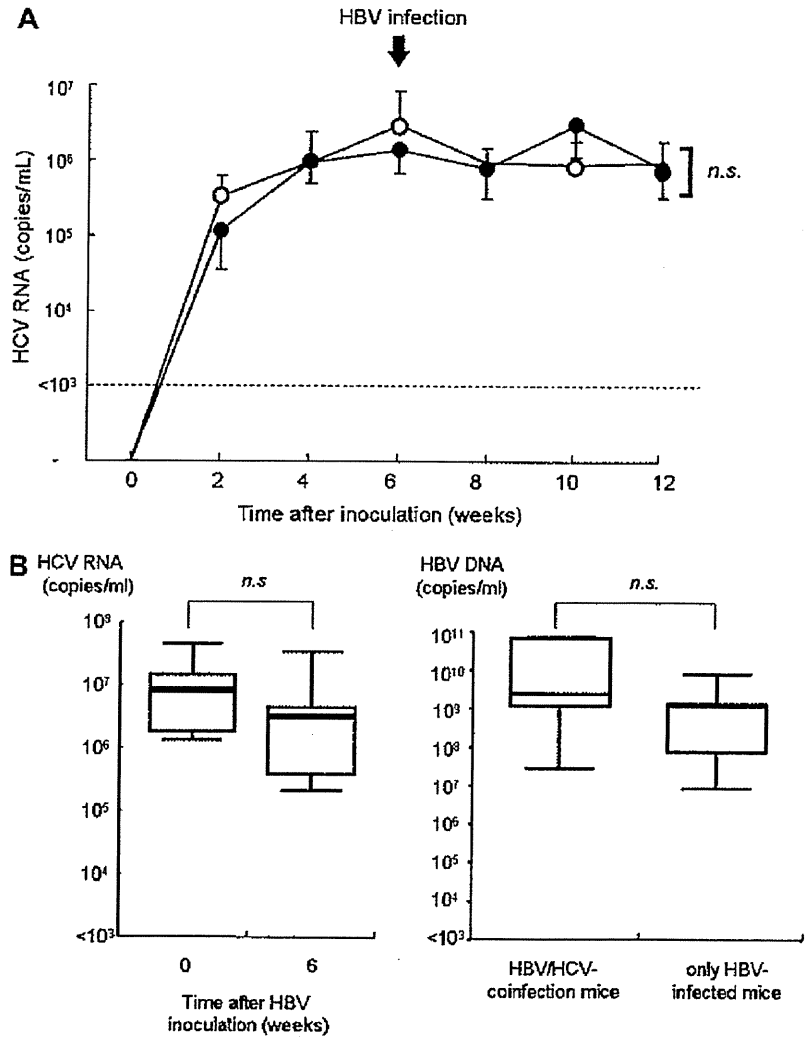

Fig. 2. Comparison of hepatitis C virus (HCV) and hepatitis B virus (HBV) titers in experimentally infected mice. (A) Ten mice were inoculated with HCV-positive serum samples. Six weeks after HCV infection, 5 of the 10 mice were inoculated with HBV-positive human serum samples (closed circles). The remaining five mice (open circles) did not receive HBV inoculation. Data are mean plus or minus standard deviation ($n = 3$). (B) Serum HCV RNA titers in five mice infected with HCV before and at 6 weeks after HBV superinfection (left panel). Serum HBV DNA titers in five mice coinfected with HBV and HCV were compared with those of five mice with HBV infection only (Fig. 1) at 12 weeks after HCV inoculation (right panel). In these box-and-whisker plots, lines within the boxes represent the median values; the upper and lower lines of the boxes represent the 25th and 75th percentiles, respectively.

Accumulation of mononuclear cells is usually seen in the livers of infected individuals, in association with the state of inflammation. It is thus difficult to examine the interference of hepatitis viruses in infection and replication in liver cells without taking into consideration the effect of these immune cells as well as the chemokines and cytokines produced by these cells. Instead, the present study was designed to examine the interference between HBV and HCV in an experimental setup lacking such inflammatory interferences. The SCID-based human hepatocyte chimeric mouse model is ideal for investigating such interaction. We expected either reduction of HCV after inoculation of HBV in HCV-infected mice or failure to develop HBV viremia or low-level HBV viremia in these mice due to viral interference; however, no reduction in HCV titers occurred in these mice, and HBV infection developed in a manner similar to that in naïve mice (Fig. 2). We thus confirmed that there is no interference between the two viruses in the absence of immune reaction via the infiltrating lymphocytes in the liver.

Wieland et al. reported that HBV did not induce any genes during entry or expansion in HBV-infected chimpanzee livers and suggested that HBV was a stealthy virus early in the infection [19]. Because no reduction in HCV was noted during and after the development of high-level HBV viremia, we assume that HBV escapes innate immunity via an excellent mechanism without

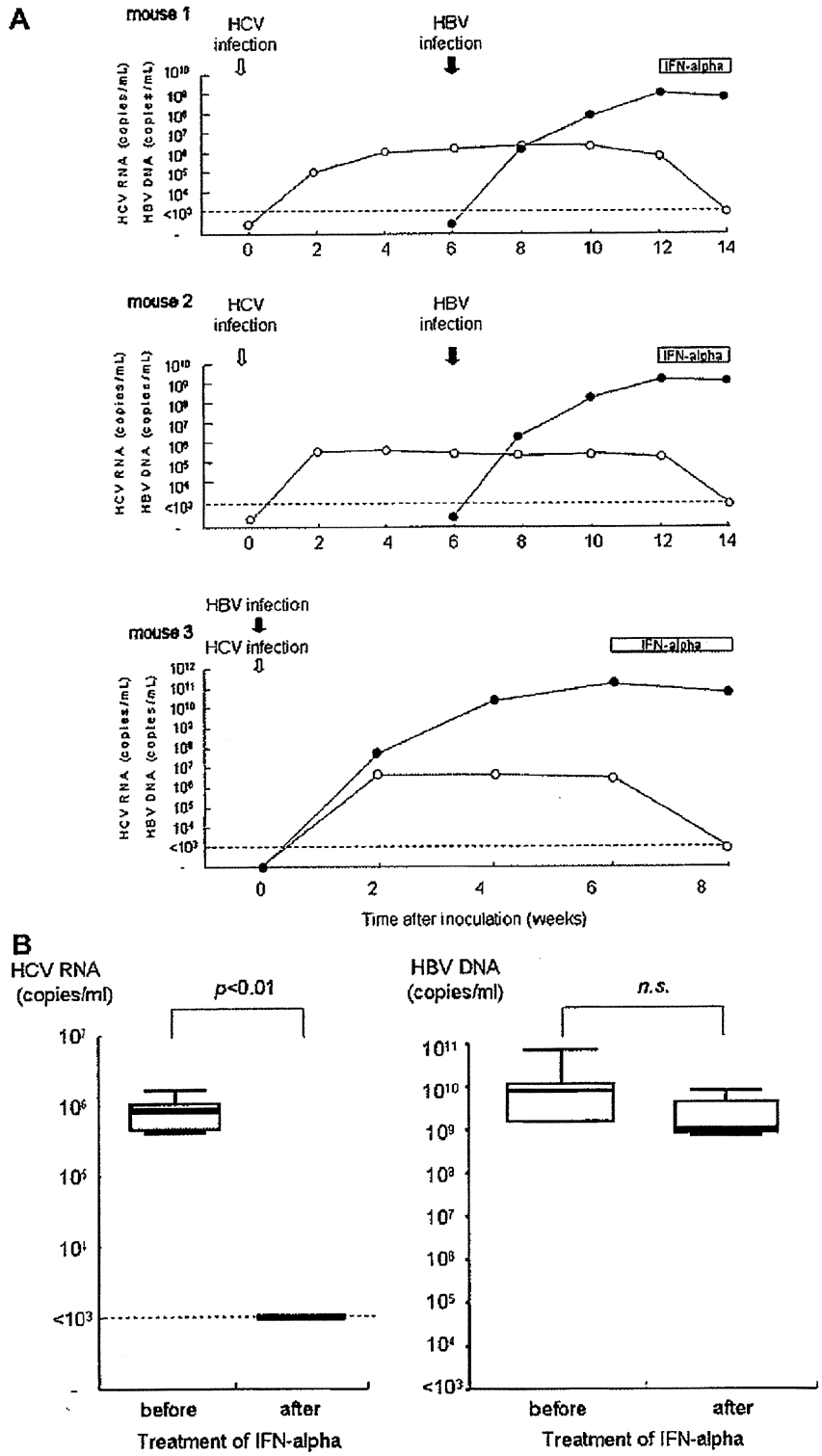

Fig. 3. Changes in serum hepatitis C virus (HCV) RNA and hepatitis B virus (HBV) DNA levels and effects of IFN on HBV–HCV-coinfected mice. Three mice (mouse 1, 2, and 3) were inoculated with both HBV- and HCV-positive human serum samples and treated daily with 7000 IU/g per day of interferon-alpha (IFN-α) intramuscularly for 2 weeks. Mice sera samples were obtained every 2 weeks after injection, and HCV RNA (open circles) and HBV DNA (close circles) were analyzed by quantitative polymerase chain reaction. (A) The horizontal dashed line represents the detectable limit (10^3 copies per milliliter). (B) Serum HCV RNA and HBV DNA titers in mice before and after 2-week IFN-α treatment. In these box-and-whisker plots, lines within the boxes represent median values; the upper and lower lines of the boxes represent the 25th and 75th percentiles, respectively.

Table 1
Hepatitis B virus (HBV) markers in supernatants of stable HBV-transfected cell lines.

Clone	HBsAg (IU/L)	HBeAg (IU/L)	HBV DNA (log copies per milliliter)
39	0.46	4.57	5.2
42	8.16	1.34	5.3
53	0.08	9.29	5.4

Abbreviations: HBsAg, hepatitis B surface antigen; HBeAg, hepatitis B e antigen.

evoking the IFN production system in liver cells. Further study using double-infected mice treated with anti-HBV nucleotide analogs and anti-HCV protease inhibitors should be conducted to confirm the present findings.

With regard to the use of IFN as a treatment, we initially assumed that HBV infection would prevent the effect of IFN on HCV and possibly vice versa in double-infection mice. Unexpectedly, the reduction of HCV by IFN therapy was quite similar in mice infected with HCV only and in those coinfected with HBV and HCV (Figs. 1 and 3). This finding indicated that HBV does not disturb the effect of IFN through signal transduction from the IFN receptor through the Jak-STAT pathway. It was, however, considered possible that HBV and HCV infect different liver cells in mice and replicated without being affected by each other. It has been reported that the same liver cell could be infected with both HBV and HCV [20,26], but it was difficult in the present study to confirm that these two viruses replicate in the same liver cell of mice because it is difficult to visualize HCV antigen and RNA in pathologic sections of the mouse liver. To address this issue, we transfected HCV to stable HBV-producing cell lines (Fig. 4). We thought that both HCV and HBV were produced from successfully HCV RNA transfected cells because transfected cells were stable HBV-producing cells. Presence of the both hepatitis viruses in the same hepatocytes has also been shown by a recent report by Bellecave et al. [20]. We showed in our cell line experiments that only HBV-transfected cell lines produced HBV and that cells cotransfected with HBV and HCV did not show a clear effect of HCV replication on HBV production (Fig. 4A). Similarly, stable production of HBV did not alter the replication of HCV (Fig. 4B). These data are consistent with a recent report [20] that showed that HCV could infect cells producing HBV and suggest a lack of interference between the two viruses in liver cells.

Using HCV-transfected HBV-producing cell lines, we demonstrated that presence of HBV did not disturb the actions of IFN on HCV (Fig. 5C). HCV utilizes certain machinery to disrupt the innate immune system; however, once exposed a large concentration of IFN, the virus shows high sensitivity, as shown in the replicon system [16,27]. Thus, HCV seems to have a relatively weak ability to disturb the antiviral actions of IFN compared with HBV. In contrast, HBV showed strong resistance against IFN in cells with diminished HCV replication [28]. The fact that HBV does not disturb IFN signaling but resists the actions of IFN suggests that HBV counteracts the actions of IFN at IFN-induced antiviral product levels.

Although the culture environment is different from the replicon system, the JFH1 strain seems relatively resistant to IFN [29]. This suggests that the core and envelope proteins, which are absent in the replicon system, might play a role in IFN resistance; however, we could not show any effect for HCV infection on the actions of IFN on HBV replication. This finding sug-

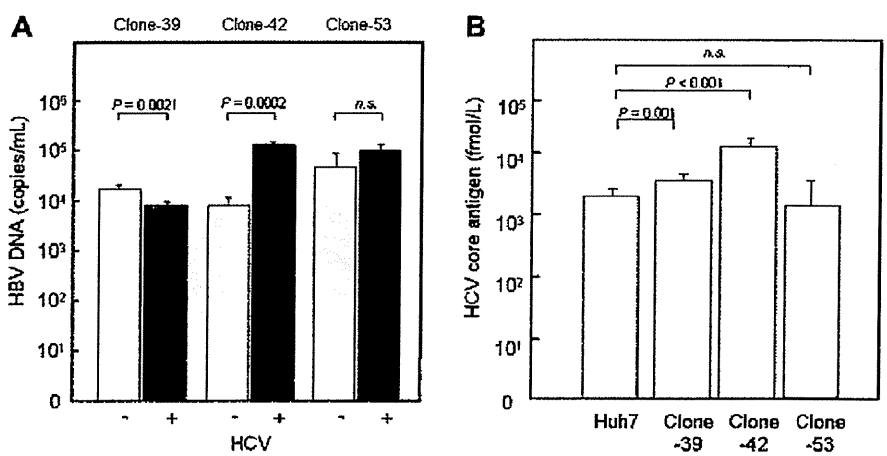

Fig. 4. Virus titers in supernatants of hepatitis B virus (HBV)–transfected or hepatitis C virus (HCV)–transfected cell lines. Huh7 cells were initially stably transfected with 1.4 genome-length HBV DNA. Three cell lines (Clone-39, -42, and -53) producing HBV DNA into the supernatant were selected. (A) HBV DNA levels in supernatants of HBV-producing cell lines 72 hours after transfection with JFH1 RNA (HCV positive) or control plasmid (HCV negative). (B) HCV core antigen levels in the supernatant of parental Huh7 cells and HBV-producing cell lines 72 h after transfection with JFH1 RNA. Data are mean plus or minus standard deviation ($n = 3$).

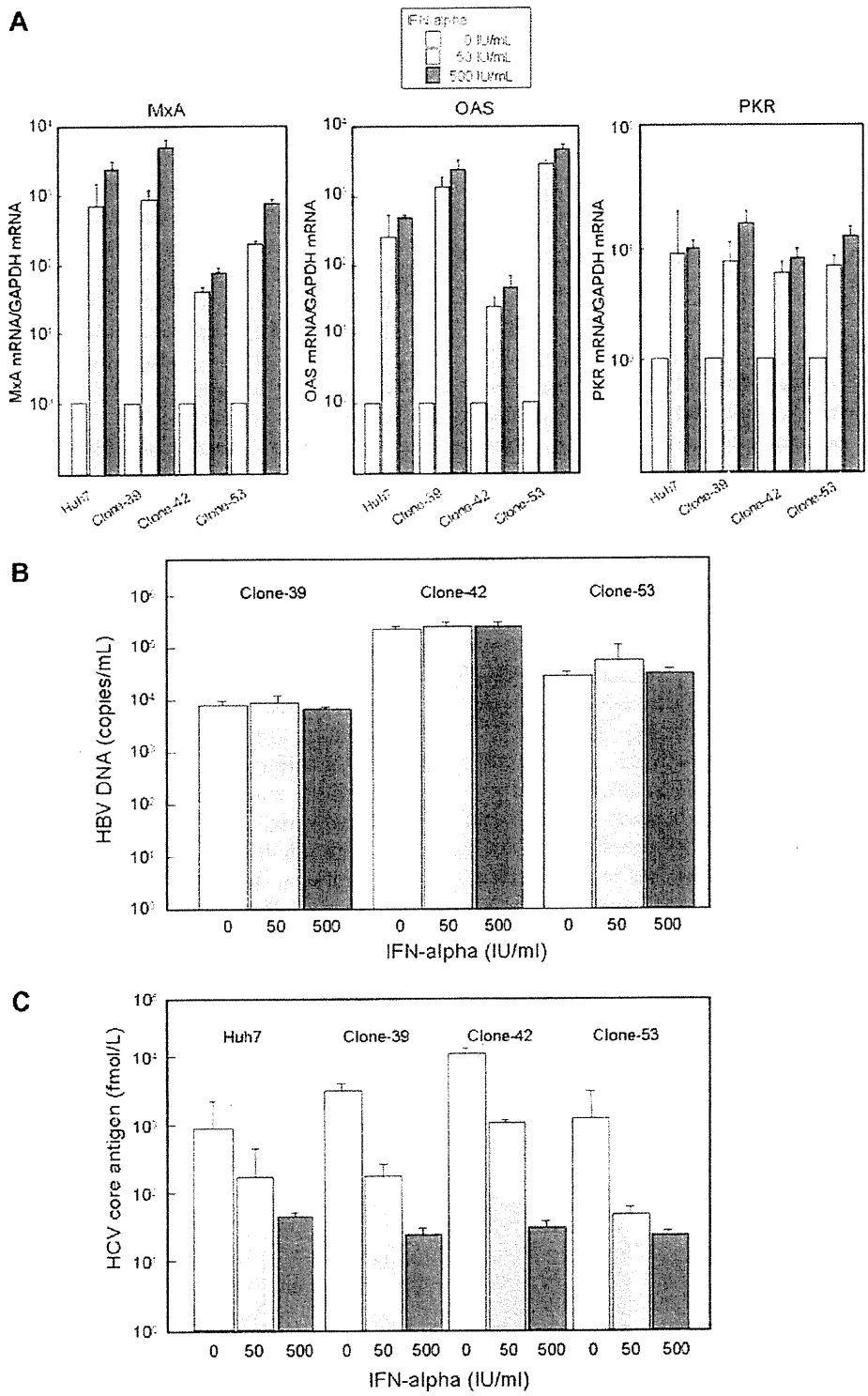

Fig. 5. Effects of interferon (IFN) treatment on hepatitis B virus (HBV) and hepatitis C virus (HCV) *in vitro*. Parental Huh7 cells and three HBV-transfected Huh7 cell lines (Clone-39, -42, and -53) were transfected with JFH1 RNA. Immediately after JFH1 transfection, the cell lines were treated with IFN-α (0, 50, and 500 IU/mL) for 72 h. (A) Intracellular gene expression levels of mixovirus resistance protein A (MxA), 2′,5′-oligoadenylate synthetase (OAS), and RNA-dependent protein kinase (PKR) were measured. RNA levels were expressed relative to glyceraldehydes-3-phosphate dehydrogenase (GAPDH) messenger RNA. (B) HBV DNA and (C) HCV core antigen in supernatants were measured. Data are mean plus or minus standard deviation ($n = 3$).

gests that the core and envelope proteins have only a weak effect on IFN resistance.

In clinical practice, HBV shows high resistance against IFN therapy. This is also the case in the cell culture system, as we showed in this study and has been reported in previous studies [20,28]. The mechanism by which hepatitis viruses resist IFN needs to be clarified in order to develop new and effective therapies for eradication of these viruses.

Acknowledgments

The authors thank Yoshie Yoshida, Kazuyo Hattori, and Rie Akiyama for their excellent technical help.

This study was supported in part by a Grant-in-Aid for Scientific Research from the Japanese Ministry of Labor and Health and Welfare.

References

[1] Maddrey WC. Hepatitis B: an important public health issue. J Med Virol 2000;61:362–366.

[2] Global surveillance and control of hepatitis C. Report of a WHO Consultation organized in collaboration with the Viral Hepatitis Prevention Board, Antwerp, Belgium. J Viral Hepat 1999;6:35–47.

[3] Beasley RP. Hepatitis B virus. The major etiology of hepatocellular carcinoma. Cancer 1988;61:1942–1956.

[4] Samuel CE. Antiviral actions of interferons. Clin Microbiol Rev 2001;14:778–809.

[5] Sagnelli E, Coppola N, Scolastico C, Filippini P, Santantonio T, Stroffolini T, et al. Virologic and clinical expressions of reciprocal inhibitory effect of hepatitis B, C, and delta viruses in patients with chronic hepatitis. Hepatology 2000;32:1106–1110.

[6] Chiaramonte M, Stroffolini T, Vian A, Stazi MA, Floreani A, Lorenzoni U, et al. Rate of incidence of hepatocellular carcinoma in patients with compensated viral cirrhosis. Cancer 1999;85:2132–2137.

[7] Cacciola I, Pollicino T, Squadrito G, Cerenzia G, Orlando ME, Raimondo G. Occult hepatitis B virus infection in patients with chronic hepatitis C liver disease. N Engl J Med 1999;341:22–26.

[8] Raimondo G, Brunetto MR, Pontisso P, Smedile A, Maina AM, Saitta C, et al. Longitudinal evaluation reveals a complex spectrum of virological profiles in hepatitis B virus/hepatitis C virus-coinfected patients. Hepatology 2006;43:100–107.

[9] Fried MW, Shiffman ML, Reddy KR, Smith C, Marinos G, Gonçales Jr FL, et al. Peginterferon alfa-2a plus ribavirin for chronic hepatitis C virus infection. N Engl J Med 2002;347:975–982.

[10] Liu CJ, Lai MY, Chao YC, Liao LY, Yang SS, Hsiao TJ, et al. Interferon alpha-2b with and without ribavirin in the treatment of hepatitis B e antigen-positive chronic hepatitis B: a randomized study. Hepatology 2006;43:742–749.

[11] Gotoh B, Komatsu T, Takeuchi K, Yokoo J. Paramyxovirus strategies for evading the interferon response. Rev Med Virol 2002;12:337–357.

[12] Evans JD, Seeger C. Cardif: a protein central to innate immunity is inactivated by the HCV NS3 serine protease. Hepatology 2006;43:615–617.

[13] Blindenbacher A, Duong FH, Hunziker L, Stutvoet ST, Wang X, Terracciano L, et al. Expression of hepatitis C virus proteins inhibits interferon alpha signaling in the liver of transgenic mice. Gastroenterology 2003;124:1465–1475.

[14] Bode JG, Ludwig S, Ehrhardt C, Albrecht U, Erhardt A, Schaper F, et al. IFN-alpha antagonistic activity of HCV core protein involves induction of suppressor of cytokine signaling-3. FASEB J 2003;17:488–490.

[15] Taylor DR, Shi ST, Romano PR, Barber GN, Lai MM. Inhibition of the interferon-inducible protein kinase PKR by HCV E2 protein. Science 1999;285:107–110.

[16] Frese M, Pietschmann T, Moradpour D, Haller O, Bartenschlager R. Interferon-alpha inhibits hepatitis C virus subgenomic RNA replication by an MxA-independent pathway. J Gen Virol 2001;82:723–733.

[17] Christen V, Duong F, Bernsmeier C, Sun D, Nassal M, Heim MH. Inhibition of alpha interferon signaling by hepatitis B virus. J Virol 2007;81:159–165.

[18] Su AI, Pezacki JP, Wodicka L, Brideau AD, Supekova L, Thimme R, et al. Genomic analysis of the host response to hepatitis C virus infection. Proc Natl Acad Sci USA 2002;99:15669–15674.

[19] Wieland S, Thimme R, Purcell RH, Chisari FV. Genomic analysis of the host response to hepatitis B virus infection. Proc Natl Acad Sci USA 2004;101:6669–6674.

[20] Bellecave P, Gouttenoire J, Gajer M, Brass V, Koutsoudakis G, Blum HE, et al. Hepatitis B and C virus coinfection: a novel model system reveals the absence of direct viral interference. Hepatology 2009;50:46–55.

[21] Tsuge M, Hiraga N, Takaishi H, Noguchi C, Oga H, Imamura M, et al. Infection of human hepatocyte chimeric mouse with genetically engineered hepatitis B virus. Hepatology 2005;42:1046–1054.

[22] Wakita T, Pietschmann T, Kato T, Date T, Miyamoto M, Zhao Z, et al. Production of infectious hepatitis C virus in tissue culture from a cloned viral genome. Nat Med 2005;11:791–796.

[23] Hiraga N, Imamura M, Tsuge M, Noguchi C, Takahashi S, Iwao E, et al. Infection of human hepatocyte chimeric mouse with genetically engineered hepatitis C virus and its susceptibility to interferon. FEBS Lett 2007;581:1983–1987.

[24] Tateno C, Yoshizane Y, Saito N, Kataoka M, Utoh R, Yamasaki C, et al. Near completely humanized liver in mice shows human-type metabolic responses to drugs. Am J Pathol 2004;165:901–912.

[25] Noguchi C, Ishino H, Tsuge M, Fujimoto Y, Imamura M, Takahashi S, et al. G to A hypermutation of hepatitis B virus. Hepatology 2005;41:626–633.

[26] Rodríguez-Iñigo E, Bartolomé J, Ortiz-Movilla N, Platero C, López-Alcorocho JM, Pardo M, et al. Hepatitis C virus (HCV) and hepatitis B virus (HBV) can coinfect the same hepatocyte in the liver of patients with chronic HCV and occult HBV infection. J Virol 2005;79:15578–15581.

[27] Blight KJ, Kolykhalov AA, Rice CM. Efficient initiation of HCV RNA replication in cell culture. Science 2000;290:1972–1974.

[28] Hayashi Y, Koike K. Interferon inhibits hepatitis B virus replication in a stable expression system of transfected viral DNA. J Virol 1989;63:2936–2940.

[29] Miyamoto M, Kato T, Date T, Mizokami M, Wakita T. Comparison between subgenomic replicons of hepatitis C virus genotypes 2a (JFH-1) and 1b (Con1 NK5.1). Intervirology 2006;49:37–43.

Approach for *in Vivo* Protein Binding of 5-*n*-Butyl-pyrazolo[1,5-*a*]pyrimidine Bioactivated in Chimeric Mice with Humanized Liver by Two-Dimensional Electrophoresis with Accelerator Mass Spectrometry

Hiroshi Yamazaki,*,† Shunji Kuribayashi,‡ Tae Inoue,§,|| Chise Tateno,§ Yasufumi Nishikura,§ Ken Oofusa,⊥ Daisuke Harada,‡ Shinsaku Naito,‡ Toru Horie,§ and Shigeru Ohta||

Showa Pharmaceutical University, Machida, Tokyo 194-8543, Japan, Preclinical Assessment Department, Otsuka Pharmaceutical Factory, Inc., Naruto, Tokushima 772-8601, Japan, PhoenixBio, Co., Higashi-Hiroshima, Hiroshima 739-0046, Japan, Graduate School of Biomedical Sciences, Hiroshima University, Minami-ku, Hiroshima 734-8553, Japan, and Towa Environment Science Co., Suminoe-ku, Osaka 559-0034, Japan

Received September 9, 2009

Drug development of a potential analgesic agent 5-*n*-butyl-7-(3,4,5-trimethoxybenzoylamino)pyrazolo[1,5-*a*]pyrimidine was withdrawn because of its limited hepatotoxic effects in humans that could not be predicted from regulatory animal or *in vitro* studies. *In vivo* formation of glutathione conjugates and covalent binding of a model compound 5-*n*-butyl-pyrazolo[1,5-*a*]pyrimidine were investigated in the present study after intravenous administration to chimeric mice with a human or rat liver because of an interesting capability of human cytochrome P450 1A2 in forming a covalently bound metabolite *in vitro*. Rapid distribution and elimination of radiolabeled 5-*n*-butyl-pyrazolo[1,5-*a*]pyrimidine in plasma or liver fractions were seen in chimeric mice after intravenous administration. However, similar covalent binding in liver was detected over 0.17−24 h after intravenous administration. Radio-LC analyses revealed that the chimeric mice with humanized liver preferentially gave the 3-hydroxylated metabolite and its glutathione conjugate in the plasma and liver. On the contrary, chimeric mice with a rat liver had some rat-specific metabolites *in vivo*. Analyses by electrophoresis with accelerator mass spectrometry of *in vivo* radiolabeled liver proteins in chimeric mice revealed that bioactivated 5-*n*-butyl-pyrazolo[1,5-*a*]-pyrimidine bound nonspecifically to a variety of microsomal proteins including human P450 1A2 as well as cytosolic proteins in the livers from chimeric mice with humanized liver. These results suggest that the hepatotoxic model compound 5-*n*-butyl-pyrazolo[1,5-*a*]pyrimidine was activated by human liver microsomal P450 1A2 to reactive intermediate(s) *in vivo* in humanized chimeric mice and could relatively nonspecifically bind to biomolecules such as P450 1A2 and other proteins.

Introduction

Cytochrome P450 comprises a superfamily of enzymes involved in the oxidation of a large number of endogenous and exogenous compounds associated with their pharmacological or toxicological actions (*1*). For example, it has been reported that drug-induced hepatotoxicity may be caused by active intermediates formed by animal and/or human P450 enzymes from a common toxicant acetaminophen (*2*) or idiosyncratic troglitazone withdrawn from the market (*3*). Species differences between experimental animals and humans in the roles of P450 enzymes in drug metabolism are determinant factors in evaluating drug toxicity (*4*).

Drug-induced liver injury has been one of the most frequent single causes of safety-related drug marketing withdrawals. In a clinical study of 5-*n*-butyl-7-(3,4,5-trimethoxybenzoylamino)pyrazolo[1,5-*a*]pyrimidine (Figure 1, OT-7100[1]) with a potential analgesic effect, limited elevations in the serum levels of asparate or alanine aminotransferase were abnormally observed in humans that could not be predicted from regulatory animal or *in vitro* studies (*5*). No apparent differences in plasma drug levels of volunteers were found between the toxic cases and other groups in our limited observations so far (*5*). The underlying molecular mechanisms are not yet fully known. However, human liver microsomal P450 1A2 was able to effectively mediate the transformation of a primary metabolite 5-*n*-butyl-pyrazolo[1,5-*a*]pyrimidine (M-5) into 3-hydroxy-5-*n*-butyl-pyrazolo[1,5-*a*]pyrimidine (M-23OH), yielding a possible quinone-imine metabolite that could bind to glutathione or liver proteins (Figure 1) (*5*).

Safety assessment of drug metabolites is proposed by potential application of genetically engineered mouse models that express human P450 enzymes (*6*). Recently, chimeric mice with humanized liver were established by transplanting human hepatocytes into a urokinase-type plasminogen activator$^{+/+}$/

* Corresponding author. Showa Pharmaceutical University, 3-3165 Higashi-tamagawa Gakuen, Machida, Tokyo 194-8543, Japan. Tel/Fax: +81-42-721-1406. E-mail: hyamazak@ac.shoyaku.ac.jp.
† Showa Pharmaceutical University.
‡ Otsuka Pharmaceutical Factory, Inc.
§ PhoenixBio Co.
|| Hiroshima University.
⊥ Towa Environment Science Co.

[1] Abbreviations: M-5, 5-*n*-butyl-pyrazolo[1,5-*a*]pyrimidine; M-22OH, 6-hydroxy-5-*n*-butyl-pyrazolo[1,5-*a*]pyrimidine; M-23OH, 3-hydroxy-5-*n*-butyl-pyrazolo[1,5-*a*]pyrimidine; OT-7100, 5-*n*-butyl-7-(3,4,5-trimethoxybenzoylamino)pyrazolo[1,5-*a*]pyrimidine.

10.1021/tx900323a
Published on Web 11/24/2009

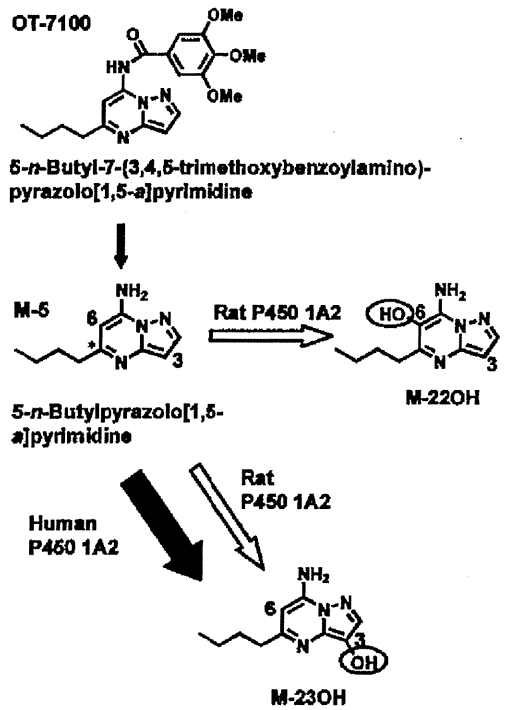

Figure 1. Metabolic fate of human hepatotoxic pyrazolopyrimidine derivative, 5-*n*-butyl-7-(3,4,5-trimethoxybenzoylamino)pyrazolo[1,5-*a*]-pyrimidine (OT-7100) and its primary metabolite 5-*n*-butyl-pyrazolo[1,5-*a*]pyrimidine (M-5), after biotransformation by human and rat P450 1A2 enzymes. Only 3-hydroxy-5-*n*-butyl-pyrazolo[1,5-*a*]pyrimidine (M-23OH) was detected in human liver microsomal incubations, but M-23OH and hydroxy-5-*n*-butyl-pyrazolo[1,5-*a*]pyrimidine (M-22OH) were seen in rat liver microsomal incubations (*5*).

severe combined immunodeficient transgenic mouse line (*7, 8*). These chimeric mice may be useful to evaluate human pharmacokinetics for developing drug candidates or idiosyncratic drugs in terms of mechanism-based adverse reactions and toxicity.

The purpose of this study was to characterize *in vivo* 5-*n*-butyl-pyrazolo[1,5-*a*]pyrimidine metabolism by human liver microsomal P450 enzymes transplanted into mice and also to better understand the activation of 5-*n*-butyl-pyrazolo[1,5-*a*]-pyrimidine and any interactions with biomolecules in the liver including covalent binding by electrophoresis analysis with accelerator mass spectrometry. In order to investigate different oxidative metabolic profiles of the species-specific hepatotoxic pyrazolopyrimidine derivative, chimeric mice with rat livers (*7, 9*) were also used and compared with mice with humanized livers. We report herein that the metabolically activated 5-*n*-butyl-pyrazolo[1,5-*a*]pyrimidine binds nonspecifically to a variety of microsomal proteins including human P450 1A2 (a bioactivating enzyme) or prolyl-4-hydroxylase as well as cytosolic proteins including catalase in chimeric mice with humanized livers.

Experimental Procedures

Chemicals and Enzymes. 5-*n*-Butyl-pyrazolo[1,5-*a*]pyrimidine (M-5) and its ^{14}C-labeled compound (the labeling position was the 5 position carbon atom in the pyrazolopyrimidine ring as shown in Figure 1), 3-hydroxy-5-*n*-butyl-pyrazolo[1,5-*a*]pyrimidine (M-23OH), 6-hydroxy-5-*n*-butyl-pyrazolo[1,5-*a*]pyrimidine (M-22OH), and 5-*n*-pentyl-7-(3,4,5-trimethoxybenzoylamino)pyrazolo[1,5-*a*]pyrimidine (OT-7126) as an internal standard for HPLC analysis were synthesized at Otsuka Pharmaceutical Factory (Tokushima, Japan). All these chemicals were determined, by reversed-phase HPLC, to be >99.0% pure. Reduced glutathione was purchased from Sigma-Aldrich (St. Louis, MO). Recombinant human and rat P450 1A2 coexpressed with NADPH-P450 reductase in baculovirus-infected insect cells (Supersomes) and antibodies against human P450 enzymes were purchased from Nosan (Yokohama, Japan) and BD Gentest (Woburn, MA). All other chemicals and reagents used were of analytical reagent grade.

Animal Experiments. Chimeric mice (PXB mice) with a human or rat liver used in this study were prepared by PhoenixBio Co. (Hiroshima, Japan) (*7, 9*). Briefly, male chimeric mice (10−14 weeks old, 15 g body weight) with human hepatocytes (male Caucasian, 2 years old from BD Biosciences, San Jose, CA) or rat hepatocytes (pooled from five male Sprague−Dawley rats, 10 weeks old were purchased from Charles River Japan, Kanagawa, Japan) were transplanted into a urokinase-type plasminogen activator $^{+/+}$/severe combined immunodeficient transgenic mouse line (20−30 days after birth). The replacement index of the mice with the human hepatocytes for estimating the humanization of the chimeric mice was determined by measuring the levels of human albumin in the mouse blood (*10*). The livers were collected and stored at −80 °C prior to use. The frozen tissues were homogenized with 5 volume of 250 mM sucrose buffer. Protein concentrations of these samples were measured by a protein assay system (Bio-Rad Laboratories, Hercules, CA).

Metabolites Measurements. A typical *in vitro* incubation mixture (0.50 mL total volume) contained recombinant human or rat P450 1A2 (20 pmol equivalent recombinant P450/mL), 50 mM potassium phosphate buffer (pH 7.4), an NADPH-generating system (0.5 mM $NADP^+$, 5 mM glucose 6-phosphate, and 1 U/mL glucose-6-phosphate dehydrogenase), and 5-*n*-butyl-pyrazolo[1,5-*a*]pyrimidine (5.0 μM) in the absence or presence of reduced glutathione (50 mM). After a 5 min preincubation, the reactions were initiated by the addition of the NADPH-generating system and were incubated at 37 °C for 30 min. The reactions were terminated by 0.50 mL of methanol, and then OT-7126 was added as an internal standard. After centrifugation at 2,000*g* for 10 min at 4 °C, the supernatant was added to 5 mM ammonium acetate at a ratio of 1:1, and a 0.20 mL aliquot was injected onto the LC system. In the case of the analysis of *in vivo* samples, a 0.2 mL aliquot of each plasma or liver homogenate sample was first added to 0.46 mL of methanol, and then OT-7126 was added as an internal standard. After centrifugation at 10,000*g* for 15 min at 4 °C, the supernatant (0.5 mL) was transferred to another tube and dried under nitrogen at 40 °C. The residue was dissolved in 0.2 mL of a mixture of methanol and 5 mM ammonium acetate at a ratio of 1:3, and a 0.15 mL aliquot was injected onto the radio-LC system.

HPLC Analysis. 5-*n*-Butyl-pyrazolo[1,5-*a*]pyrimidine and its metabolites were assayed using UV-LC and radio-LC methods validated over a concentration range of 0.10−10.0 μM. 5-*n*-Butyl-pyrazolo[1,5-*a*]pyrimidine and its metabolites in incubation mixtures or plasma and liver homogenates of the chimeric mice were separated on a 250 mm × 4.6 mm i.d. Inertsil ODS-3 V column (GL-Sciences, Tokyo, Japan) and detected at wavelengths of 230 nm or by FLO-ONE/Beta Model A525 as a radio-detector using an HPLC system (LC-10A Series, Shimadzu, Kyoto, Japan). The column temperature was maintained at 40 °C. The mobile phase was 5 mM ammonium acetate (A) and acetonitrile (B). The conditions for elution were as follows: 13 to 25% B (0−8 min), 25 to 25% B (8−20 min), 25 to 35% B (20−25 min), 35 to 80% B (25−31 min), and 80 to 80% B (31−40 min). Linear gradients were used for all solvent changes. The flow rate was 0.80 mL/min in LC assays in combination with the scintillator (Ultima-Flo, PerkinElmer, Waltham, MA, at a flow rate of 2.4 mL/min) in the radio-LC assay.

Covalent Binding of Metabolically Activated Derivatives to the Liver *in Vivo*. A sodium dodecyl sulfate (SDS)−polyacrylamide gel electrophoretogram in 12% acrylamide gels with liver microsomes (10 μg) from humanized mice treated with 5-*n*-butyl-pyrazolo[1,5-*a*]pyrimidine (*5, 11*) was stained with 0.08% Coomassie Brilliant Blue R350 (GE Healthcare Bio-Science) according to the manufacturer's protocol. Radioactivity contents of each band

on the gel were determined by BAS-5000 Image Analysis System (Fujifilm, Tokyo, Japan). In separate experiments, 10 gel pieces were sliced-out by hand at 1 mm width at 35−100 kDa range from the gel after electrophoresis and were subjected to mass spectrometry for detecting P450 enzymes. In other experiments, corresponding human P450 enzymes in liver microsomes separated on the gel were also detected with anti-P450 antibodies.

Protein samples (100 μg) were applied overnight to Immobiline Drystrip (GE Healthcare Bio-Science) by in-gel rehydration as described previously (*12, 13*). After rehydrated gels were gently dried, isoelectric focusing was performed in a Pharmacia Hoefer Multiphor II electrophoresis chamber (GE Healthcare, Buckinghamshire, U.K.) according to the manufacturer's instructions. Second dimension SDS−polyacrylamide gel electrophoresis (PAGE) was performed in 9−18% acrylamide gradient gels using a IsoDalt electrophoresis chamber. The second dimension gels were stained with SYPRO Ruby (Invitrogen, Carlsbad, CA) under the manufacturer's protocols (*14*). The SYPRO Ruby-stained proteins were detected using Molecular Imager FX (Bio-Rad Laboratories, Hercules, CA) and were subjected to in-gel digestion image analysis. Database management and image analysis were done using Image Master Platinum image analysis software (GE Healthcare).

In-gel digestion and mass spectrometric identification of proteins were performed essentially as described elsewhere (*15*). Briefly, protein spots were excised from the dried silver stained second dimension gels and rehydrated for 20 min in 100 mM NH_4HCO_3. The gel spots were then destained for 20 min in a solution of 15 mM potassium ferricyanide and 50 mM thiosulfate (*16*), rinsed twice in water, and finally dehydrated in 100% acetonitrile until they turned opaque white. The spots were then dried in a vacuum centrifuge and subsequently rehydrated in a digestion solution consisting of 50 mM NH_4HCO_3, 5 mM $CaCl_2$, and 0.1 μg/μL modified sequence-grade trypsin (Promega, Madison, WI). After overnight incubation at 37 °C, the digestion was terminated in 5% trifluoroacetic acid for 20 min. Peptides were extracted 3 times (20 min each) with 5% trifluoroacetic acid in 50% acetonitrile, and the extracted peptides were pooled and dried in a vacuum centrifuge. The peptides were purified with ZipTip (Millipore, Billerica, MA) under the manufacturer's protocol and analyzed by MACOT database software (Matrix Science, Tokyo, Japan). Accelerator mass spectrometry analyses were performed with a NEC 1.5SDH-1 0.6MV Pelletron AMS system (National Electrostatics Corporation, Tokyo, Japan) to determine $^{14}C/^{12}C$ content ratio in the biological samples after dilution as described previously (*17*).

Kinetic Data Analysis. The radioactive concentrations at time 0 (C_0) were extrapolated from the initial slope. The times to reach the elimination half-lives ($t_{1/2}$) were estimated as ln 2/k, where k is the slope of the terminal linear portion of the semilogarithmic plasma concentration−time curve. The areas under the plasma concentration−time curves from time 0 to the last detectable concentration ($AUC_{0\text{-}t}$), area under the plasma concentration−time curves from time 0 to the infinite time after administration ($AUC_{0\text{-}\infty}$), and the mean residence times (MRT) were calculated. Total systemic clearances (CL_{tot}), volume of distribution (Vd), and volume of distribution at steady state ($Vdss$) were calculated according to the following equations: $CL_{tot} = D/AUC_{0\text{-}\infty}$, $Vd = D/C_0$, $Vdss = MRT{\cdot}CL_{tot} = D{\cdot}MRT/AUC_{0\text{-}\infty}$, where D is the administered dose.

Results

***In Vitro* Formation of Glutathione Conjugates of 5-*n*-Butyl-pyrazolo[1,5-*a*]pyrimidine Catalyzed by Recombinant Human or Rat P450 1A2.** Recombinant human or rat P450 1A2 was incubated with 5-*n*-butyl-pyrazolo[1,5-*a*]pyrimidine for 30 min with an NADPH-generating system and/or reduced glutathione (5.0 mM). Human P450 1A2 preferentially metabolized 5-*n*-butyl-pyrazolo[1,5-*a*]pyrimidine to M-23OH (peak 4, a C-3-position hydroxyl derivative) at substrate concentrations of 5.0 μM (Figure 2A). On the contrary, rat P450 1A2 rapidly metabolized 5-*n*-butyl-pyrazolo[1,5-*a*]pyrimidine to M-23OH, M-22OH (peak 3, a C-6-position hydroxyl derivative), or an unknown metabolite (peak 2, Figure 2C). An M-23OH-glutathione conjugate (peak 1) was also detected in the presence of glutathione and NADPH after the incubation of 5-*n*-butyl-pyrazolo[1,5-*a*]pyrimidine by P450 1A2 systems (Figure 2B,D).

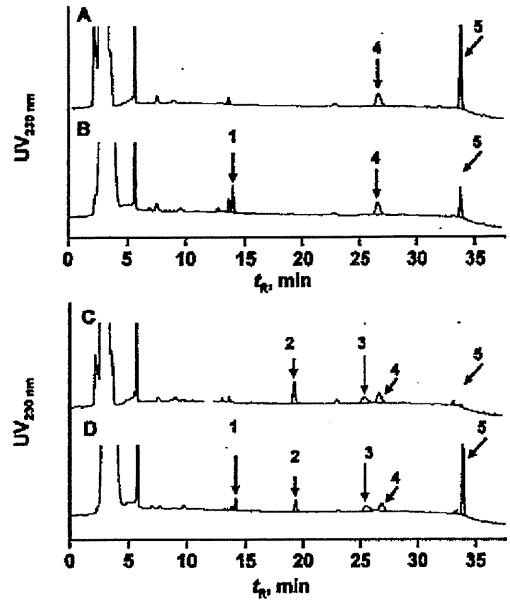

Figure 2. Representative UV-LC chromatograms of *in vitro* metabolites from 5-*n*-butyl-pyrazolo[1,5-*a*]pyrimidine (M-5) by incubation with human P450 1A2 (A,B) and rat P450 1A2 (C,D) in the absence (A,C) and presence (B,D) of reduced glutathione. Recombinant human or rat P450 1A2 (20 pmol/mL) was incubated with 5 μM 5-*n*-butyl-pyrazolo[1,5-*a*]pyrimidine (M-5) for 30 min with an NADPH-generating system and/or reduced glutathione (50 mM). Peak 1, a glutathione conjugate of M-23OH; peak 2, a rat-specific unknown product; peak 3, M-22OH; peak 4, M-23OH; and peak 5, 5-*n*-butyl-pyrazolo[1,5-*a*]-pyrimidine (M-5).

***In Vivo* Formation of Glutathione Conjugates of 5-*n*-Butyl-pyrazolo[1,5-*a*]pyrimidine after Intravenous Administration to Chimeric Mice with Human or Rat Livers.** To see *in vivo* species differences found in the 5-*n*-butyl-pyrazolo[1,5-*a*]pyrimidine metabolism *in vitro*, 5-*n*-butyl-pyrazolo[1,5-*a*]pyrimidine metabolism was investigated using chimeric mice with human or rat livers. After the administration of ^{14}C-5-*n*-butyl-pyrazolo[1,5-*a*]pyrimidine at 3 mg dose/kg body weight to chimeric mice, similar elimination curves of radioactivities in plasma were obtained in chimeric mice with a human and rat liver (Figure 3A). Similar elimination profiles were also seen in normal rats (not shown). The apparently similar pharmacokinetic parameters for radioactivity after intravenous administration of ^{14}C-5-*n*-butyl-pyrazolo[1,5-*a*]pyrimidine were obtained in chimeric mice with human or rat livers as shown in Table 1. The radioactivities were rapidly eliminated from the plasma of chimeric mice: half-lives of α- and β-elimination phases were 0.31 ± 0.06 h (mean ± SD) and 6.17 ± 1.28 h in chimeric mice with human livers. Similarly, rapid distribution (at 0.17 h after administration) and elimination (at 24 h) of radioactivity in liver fractions were seen in chimeric mice with human or rat livers after intravenous administration (Figure 3B). However, similar levels of covalent binding in livers were detected over 0.17−24 h both in chimeric mice with human and rat livers (Figure 3C).

Radio-LC assays revealed that the chimeric mice with human livers preferentially gave the M-23OH metabolite from 5-*n*-butyl-pyrazolo[1,5-*a*]pyrimidine in the liver (Figure 4C) and an M-23OH-glutathione conjugate in the plasma (Figures 4A). The

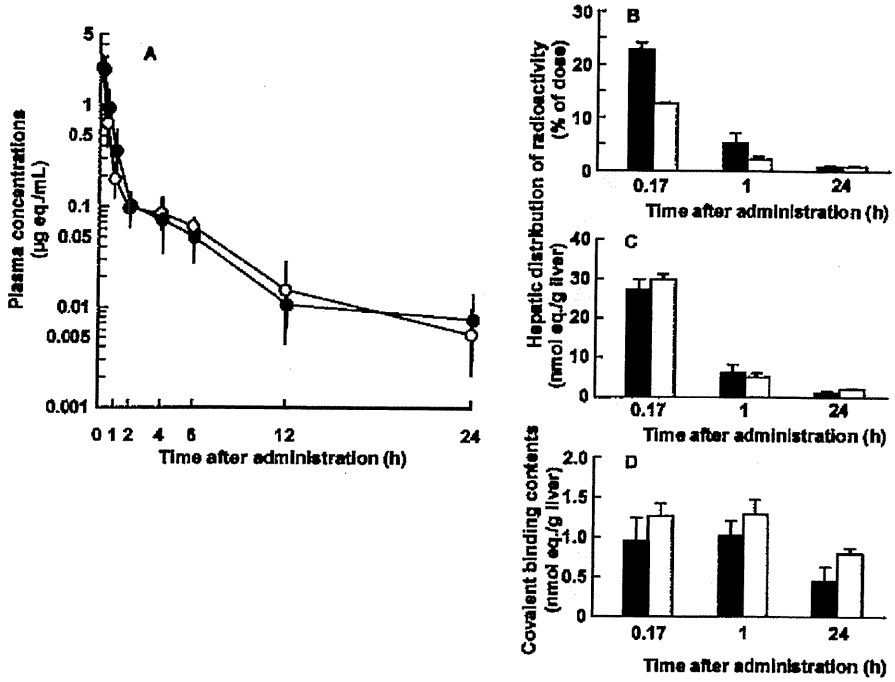

Figure 3. Plasma (A) or liver (B,C) concentrations of radiolabeled 5-*n*-butyl-pyrazolo[1,5-*a*]pyrimidine (M-5) and covalent protein binding to liver fractions (D) in chimeric mice with human (●, ■) or rat (○, □) livers after intravenous administration. ^{14}C-5-*n*-Butyl-pyrazolo[1,5-*a*]pyrimidine was administered intravenously at a dose of 3.0 mg/kg in the chimeric mice. Results are expressed as the mean values ± SD of three mice.

Table 1. Animal Profiles and Pharmacokinetic Parameters of Plasma Radioactivity Levels of Human- or Rat-Chimeric Mice after Intravenous Administration of 3.0 mg/kg of ^{14}C-5-*n*-Butyl-pyrazolo[1,5-*a*]pyrimidine (M-5)[a]

	chimeric mice with	
	human liver	rat liver
body weight (g)	20.9 ± 0.8	24.2 ± 1.7
liver weight (g)	2.27 ± 0.18	1.50 ± 0.14
extent of the replacement from mice to humans (%)	85.8 ± 7.0	
albumin concentrations in plasma (mg/mL)	8.43 ± 2.57	8.20 ± 2.43
C_0 (μg equiv/mL)	3.11 ± 0.44	3.52 ± 0.61
$AUC_{0\text{-}t}$ (μg equiv/mL·h)	2.11 ± 0.40	2.04 ± 0.28
$AUC_{0\text{-}\infty}$ (μg equiv/mL·h)	2.16 ± 0.41	2.06 ± 0.29
$t_{1/2}\alpha$ (h)	0.31 ± 0.06	0.23 ± 0.01
$t_{1/2}\beta$ (h)	6.17 ± 1.28	4.79 ± 0.26
CL_{tot} (L/h/kg)	1.42 ± 0.28	1.47 ± 0.22
Vd (L/kg)	0.98 ± 0.13	0.87 ± 0.17
MRT (h)	3.06 ± 0.64	2.98 ± 0.42
Vdss (L/kg)	4.40 ± 1.52	4.45 ± 1.28

[a] C_0, concentrations at time 0; $AUC_{0\text{-}t}$, areas under the plasma concentration−time curves from time 0 to the last detectable concentration; $AUC_{0\text{-}\infty}$, area under the plasma concentration−time curves from time 0 to the infinite time after administration; $t_{1/2}$, half-life; CL_{tot}, total systemic clearances; *Vd*, volume of distribution; *MRT*, mean residence times; *Vdss*, volume of distribution at steady state. See Experimental Procedures for details. Data are the means (±SD) from three mice.

M-23OH-glutathione conjugate was detected at almost the background level or a minor level in the liver (Figure 4C). On the contrary, chimeric mice with rat livers had the rat-specific metabolite peak corresponding to an unknown metabolite in the chromatograms obtained from the plasma and liver *in vivo* (Figure 4B,D), like the *in vitro* rat P450 1A2 system (Figure 2C,D).

Analysis of *in Vivo* Covalent Binding of 5-*n*-Butyl-pyrazolo[1,5-*a*]pyrimidine to Liver Microsomal or Cytosolic Proteins in Chimeric Mice with Human Livers. Covalent binding of 5-*n*-butyl-pyrazolo[1,5-*a*]pyrimidine in liver microsomal

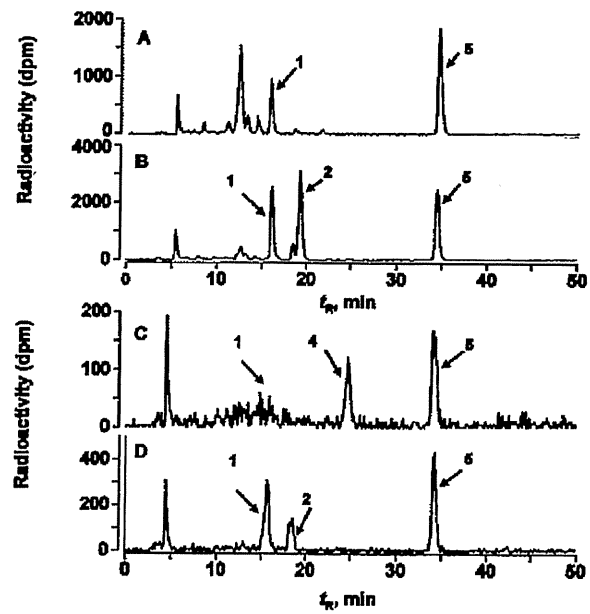

Figure 4. Representative radio-LC chromatograms of *in vivo* metabolites of radiolabeled 5-*n*-butyl-pyrazolo[1,5-*a*]pyrimidine (M-5) in plasma (A,B) and livers (C,D) at 10 min after intravenous administration to chimeric mice with human (A,C) or rat (B,D) livers. Peaks 1−5 shown here are the same as those described in the legend for Figure 2: peak 1, a glutathione conjugate of M-23OH; peak 2, a rat-specific unknown product; peak 4, M-23OH; and peak 5, 5-*n*-butyl-pyrazolo[1,5-*a*]pyrimidine (M-5).

proteins from the chimeric mice with human livers after the administration of ^{14}C-5-*n*-butyl-pyrazolo[1,5-*a*]pyrimidine was analyzed first by SDS−PAGE. As shown in Figure 5A, many bands existed in the gel after Coomassie blue staining: 10 protein bands in the ranges of 35−100 kDa in the liver microsomes were focused. After measurements of protein contents (Figure 5B) and radioactivities (Figure 5C) of the 10 analyte pieces, specific covalent binding of 5-*n*-butyl-pyrazolo[1,5-*a*]pyrimidine

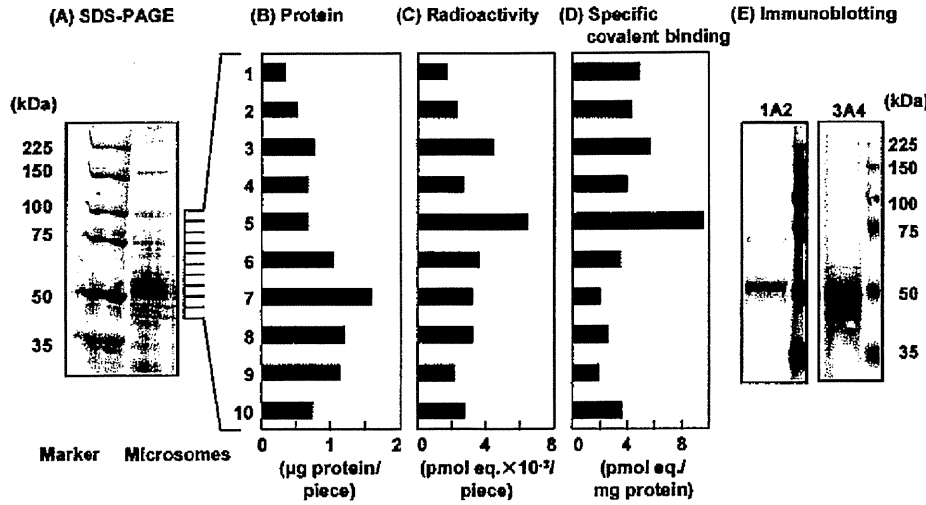

Figure 5. Covalent binding analysis after SDS−PAGE of liver microsomal proteins obtained from chimeric mice with humanized liver after the administration of radiolabeled 5-*n*-butyl-pyrazolo[1,5-*a*]pyrimidine (M-5). SDS−polyacrylamide gel electrophoretogram (A) was stained with Coomassie Brilliant Blue. Protein (B) and radioactivity (C) contents of each piece on the gel were determined. Specific covalent binding contents were expressed as pmol 5-*n*-butyl-pyrazolo[1,5-*a*]pyrimidine bound per mg microsomal protein (D).

was calculated (Figure 5D). Approximately 2−10 pmol equivalents of 5-*n*-butyl-pyrazolo[1,5-*a*]pyrimidine bound to a variety of liver microsomal proteins per mg total microsomal protein. The radioactivities from metabolically activated 5-*n*-butyl-pyrazolo[1,5-*a*]pyrimidine bound to human P450 1A2 (fraction 7, Figure 5E), P450 3A4 (fraction 8, Figure 5E), and other many microsomal proteins including P450 2C9, 2C19, and 2D6 in humanized livers were judged from immunoblotting and molecular weights on the gel.

Covalent binding profiles of liver microsomal and cytosolic fractions were further investigated by two-dimensional electrophoresis in the chimeric mice with humanized livers after the administration of radiolabeled 5-*n*-butyl-pyrazolo[1,5-*a*]pyrimidine. Protein samples (100 μg) were separated by isoelectric points (pH 3−10) and molecular weight (10−225 kDa) (Figure 6A,B). Protein contents and covalent binding contents of these analyte spots in the gels were determined. Two-dimensional electrophoresis associated with accelerator mass spectrometry analyses revealed that 5-*n*-butyl-pyrazolo[1,5-*a*]pyrimidine bound covalently to a variety of liver microsomal (Figure 6C) and cytosolic (Figure 6D) proteins. The highest specific binding was observed in prolyl-4-hydroxylase (0.016 pmol equiv/μg protein, a key enzyme in the biosynthesis of collagens) in microsomal proteins (a spot of 0.15 μg protein/mg microsomal protein shown in Figure 6C) and an antioxidant enzyme catalase (0.0099 pmol equiv/μg protein, a spot of 1.26 μg protein/mg cytosolic protein shown in Figure 6D) in cytosolic proteins, respectively, after two-dimensional electrophoresis and accelerator mass spectrometry analysis.

Discussion

Idiosyncratic drug toxicity like hepatotoxicity is a major complication of drug therapy and drug development. Many idiosyncratic reactions appear to have an immunological etiology with increasing evidence for the role of T-lymphocytes (*18*). Toxicity testing has been ineffective in the prediction of drug candidates that will be associated with a relatively high incidence of idiosyncratic drug reactions. Circumstantial evidence suggests the involvement of reactive metabolites in the etiology of these reactions, and this has prompted several companies to screen drug candidates for the formation of such compounds (*19*). It has been suggested that bioactivated small organic molecules *in vivo* resulting in electrophiles can adduct to biological macromolecules (approximately 1 nmol drug equiv/mg protein) and subsequently elicit organ toxicity (*20*). To reduce this figure by 20-fold gave a conservative target threshold value for *in vivo* covalent binding of 50 pmol drug equiv/mg protein (*20*). *In vitro* covalent binding analysis of drug candidates bioactivated by human liver microsomes is generally available for safety tests (*20*). To develop efficient prediction methods, a better understanding of the basic mechanisms involved is essential. Established chimeric mice with humanized livers (*7, 8*) would be good predictors compared with human liver microsomes because these livers have both microsomal and cytosolic enzyme systems for understanding whole drug metabolism and disposition *in vivo*. In our analysis for the evaluation of drug−protein adducts *in vivo*, a new approach by electrophoresis associated with accelerator mass spectrometry was first adapted. The low but measurable radioactivity in separated spots on the gel determined by accelerator mass spectrometry in this study could yield a new evaluation system for the drug-target proteins (as discussed below).

The present target compound 5-*n*-butyl-pyrazolo[1,5-*a*]pyrimidine (Figure 1) is the primary metabolite of a previous drug candidate, 5-*n*-butyl-7-(3,4,5-trimethoxybenzoylamino)pyrazolo[1,5-*a*]pyrimidine, with a potential analgesic effect (*5*). Bioactivation of this model compound was effectively catalyzed by recombinant human P450 1A2 (Figure 2) *in vitro* and also by livers in humanized mice *in vivo* through C^3-hydroxylation to form covalent protein binding (Figure 3) and a glutathione adduct (Figure 4). On the contrary, chimeric mice with rat livers had some rat-specific metabolites *in vivo* (Figure 4). These results demonstrated that livers of the chimeric mice with humanized livers could activate 5-*n*-butyl-pyrazolo[1,5-*a*]pyrimidine *in vivo*, leading to human-selective covalent binding and that the *in vivo* metabolic pattern of 5-*n*-butyl-pyrazolo[1,5-*a*]-pyrimidine was the same as that of *in vitro* metabolites in human liver microsomes (*5*) or recombinant human P450 1A2 shown here by radio-LC systems.

Profiles of the drug−protein adducts from bioactivated 5-*n*-butyl-pyrazolo[1,5-*a*]pyrimidine were analyzed by separations with SDS−PAGE (Figure 5) and two-dimensional electrophoresis (Figure 6). P450 1A2 in humanized liver was capable of oxidizing 5-*n*-butyl-pyrazolo[1,5-*a*]pyrimidine at the C^3-position